People's Democratic Republic of Algeria

Ministry of higher Education and
Scientific Research

University Echahid Hamma Lakhdar of El-Oued
Faculty of Technology

Report Presented in Partial Fulfilment

Of the Requirements of the

MASTER ACADEMIC

Domain: Technology
Option: Electrical Engineering
Specialist: Electrics Machines

Thesis

Sensorless Optimal Power Control of Doubly Fed Induction Generator in Variable Speed Wind Turbine System

Supervised by:
Dr. SEHOUD Hicham

Realised by:
LAMA Abdelbadia

University year: 2018/2019

Abstract

The present work is an aims to study a sensorless power control of the doubly fed induction generator (DFIG) in wind energy conversion system (WECS) without speed sensors based of application of the MRAS technique for estimation of rotor speed, the stator flux oriented vector control (technique) is used for control active and reactive power. The simulation results in MATLAB/Simulink platform verify the good static and dynamic performance of this sensorless power control for DFIG in variable speed wind turbines.

Keywords

Doubly fed induction generator (DFIG), Vector control, PWM converter, Maximum power point tracking (MPPT), MRAS observer.

Résumé

Le travail présent la commande vectorielle sans capteur mécanique de la machine asynchrone à double alimentation (MADA) intégrée dans un système éolien basé sur un système adaptatif à modèle de référence (MRAS). La commande vectorielle par orientation de flux statorique est utilisé pour contrôlé la puissance active et la puissance réactive. Les résultats de simulation numériques à base du logiciel Matlab/Simulink vérifié les bonnes performances statiques et dynamiques de cette commande.

Mots clés:

GADA, Commande vectorielle sans capteur, convertisseur MLI, Commande MPPT, Observateur MRAS.

التّلخيص:

يهدف العمل الحالي إلى دراسة التحكم في الطاقة بدون مستشعر لمولد هوائي لا تزامني مزدوج التغذية في نظام تحويل طاقة الرياح بدون مستشعرات السرعة استنادًا إلى تطبيق تقنية نظام التكيف المرجعي النموذجيMRAS لتقدير سرعة الدوار، التحكّم في الإشعاع الموجّه لتدفق الجزء الثابت استخدم في تقنية التحكم للسيطرة على القوة النشطة والتفاعلية.

تحقق نتائج المحاكاة التي تم إنجازها تحت بيئةMatlab/Simulink من الأداء الثابت والديناميكي لعنصر التحكم في الطاقة بدون مستشعر من أجل مولد هوائي لا تزامني مزدوج التغذية في توربينات الرياح السريعة المتغيرة.

كلمات مفتاحية:

طاقة الرياح ,المولد اللا تزامني مزدوج التغذية, التحكم الشعاعي عن طريق توجيه التدفق, المحول PWM, نظام التكيف المرجعي النموذجي MRAS, العنفة الهوائية وتحكمها MPPT.

Acknowledgements

First, and foremost, I would like to express my deepest appreciation to our academic advisor Dr. SERHOUD Hicham for his time, expertise and knowledge that they have given to me during the preparation of this thesis. It has been a privilege to work under his supervision.

I would also like to thank my parents who have always supported and believed in me. God bless them.

Thanks also to my family, wife, as they always understood when I was working and unable to give attention to her and my children.

Finely, Thanks are also to many of my friends and colleagues who have encouraged and supported me during study time.

Abstract i

Acknowledgement ii

Table of Contents iii

List of Symbols vi

List of Figures viii

List of Tables x

General Introduction 1

Chapter 1: Basics of Wind Power Generation System

1.1. Introduction……..3

1.2. Renewable energy development..……..…….3

1.3. Wind energy development..…….4

1.4. Basic structure of a wind turbine...……..5

1.5. Classification of wind turbine ……..…….....6

1.5.1. Vertical axis wind turbine (VAWT)..……6

1.5.2. Horizontal axis wind turbines (HAWT)..……..……7

1.5.3. Number of blades...….....…….8

1.5.4. Betz limit...……..……..…….....8

1.5.5. Upwind and downwind turbines..……..9

1.6. Wind energy conversion……...……9

1.6.1. Aerodynamic power control.…….....10

1.6.1.1. Pitch control…...…….....10

1.6.1.2. Passive stall regulation……...……..11

1.6.1.3 Active stall regulation...…….……..12

1.7. Wind energy conversion system configurations….....13

1.7.1. Fixed speed wind turbine...…….....14

1.7.2. Variable speed wind turbine with reduced capacity converters...……...14

1.7.2.1. Wound rotor induction generator with variable rotor resistance...……...15

1.7.2.2. Doubly fed induction generator with rotor converter…….…….....16

1.7.3. Variable speed wind turbine with full capacity power converters…….....16

1.8. Advantages and disadvantages of wind energy.……17

1.8.1. Advantages of wind energy……..……...17

1.8.2. Disadvantages of wind energy…..……..……18
1.9. Conclusion...……...18

Chapter 2: Modeling and Vector Control of DFIG

2.1. Introduction……19
2.2. Components of DFIG…….....…..……..19
2.3. Principle of operation of DFIG……..20
2.3.1. Sub-synchronous mode of operation....……...20
2.3.2 Super-synchronous mode of operation…….…….....21
2.4. Advantages and disadvantages of the DFIG……...22
2.4.1. Advantages of the DFIG……..……..……..22
2.4.2. Disadvantages of the DFIG.....……..23
2.5. Modeling of DFIG...……..…….....23
2.5.1. Simplifying assumptions..…….……...……...23
2.5.2. Mathematical model of doubly fed induction generator…….....……23
2.5.2.1. Electrical equation of DFIG.....…….…..……..23
2.5.2.2. Magnetic equations…….…….....24
2.5.2.3. Mechanical equations …….……25
2.5.3. Doubly fed induction generator model (d-q model)..…….....25
2.5.3.1. Park transformation.....…….……...……..25
2.5.3.2. Voltages equation...…….……...……..26
2.5.3.3. Flux equation.……..…….....27
2.5.3.4. Electromagnetic torque equation.....27
2.5.3.5. Active and reactive power equations……...……...……28
2.6. Fundamentals of vector control of induction machines.....…….……...……28
2.7. Vector control of doubly fed induction generator…….…..….....29
2.7.1. Stator field oriented of the DFIG……...…..…..……..…….29
2.7.2. Control of the rotor side converter (RSC)…...…….……...30
2.7.2.1. Relation between stator and rotor currents…...…...……...……..31
2.7.2.2. Expression of rotor voltage with function of rotor current ……...……..31
2.7.2.3. Expression of active and reactive power of synchronous frame……...……..32
2.7.3. Control of the grid side converter…...……...……...……...…….33
2.7.3.1. Phase locked loop (PLL) type estimator……...……...…….....34
2.8. Simulation results……...……...……...……...……...…….....35

2.9. Conclusion...……...37

Chapter 3: MPPT Control for the Proposed Wind Turbine System

3.1. Introduction……38
3.2. Modeling of wind turbine…..…..…….....38
3.2.1. The wind velocity……...…….38
3.2.2. Power recoverable by a turbine……..…….38
3.2.3. The power coefficient……...…….....40
3.2.4. Model of multiplier……. 40
3.2.5. Dynamic equation of shaft…..……..……..…….41
3.3. Scheme of turbine model..…….....41
3.4. Control strategy of turbine……..…….....42
3.5. Algorithms for maximizing extracted power…….…….43
3.6. Simulation results…….....44
3.7. Conclusion...……...47

Chapter 4: Sensorless Control of DFIG using MRAS

4.1. Introduction……48
4.2. The different methods of estimating the mechanical speed ……...48
4.2.1. Estimation of the speed with the machine model……..……..48
4.2.2. Estimation of the speed without machine model……...……..49
4.3. Sensorless control of DFIG system using MRAS observer…….....50
4.3.1. The MRAS method…….50
4.3.2. MRAS estimation of mechanical quantities of DFIG….……..……...51
4.4. Global scheme of the vector control of DFIG without sensors……..53
4.5. Simulation results..……...…….....53
4.6 Conclusion……...…….....…….56

General Conclusion.....57

Appendices 58

Bibliography.....62

List of Symbols

MRAS	Model reference adaptive system,
DFIG	Doubly Fed induction generator,
GSC	Grid side converter,
RSC	Rotor side converter,
PWM	Pulse width modulation,
MPPT	Maximum power point tracking,
WECS	Wind energy conversion system,
HAWT	Horizontal axis wind turbine,
VAWT	Vertical axis wind turbine,
SCIG	Squirrel cage induction generator,
WRIG	Wound rotor induction generator,
PMSG	Permanent Magnet synchronous generator,
PCC	Point of common coupling,
PI	Proportional integral control
AC	Alternative current,
DC	Direct current,
VSIG	Variable speed induction generator,
FSIG	Fixed speed induction generator,
v_{ds}, v_{qs}	d-q axis stator voltage,
v_{dr}, v_{qr}	d-q axis rotor voltage,
$\psi_s, \psi r$	Stator and rotor flux linkages,

M	Machine magnetising inductance,
L_s, L_r	Stator and rotor per phase winding inductances,
R_s, R_r	Stator and rotor per phase winding resistances,
P_s, P_r	Stator and rotor active power,
Q_s, Q_r	Stator and rotor reactive power,
p	Number of machine pair of pole,
Te	Electromagnetic torque,
$Tair$	Aerodynamic torque,
ω_s	Synchronous rotational speed,
ω_r	Rotor electrical speed,
θ_r	Rotor electrical angle,
θ_r	Rotor electrical angle,

Suffixes, Superscripts

s, r	stator, rotor,
α, β	α, β stationary reference frame,
d, q	d, q reference frame,
a, b, c	Three-phase reference,
$*$	Reference value.

List of Figures

Figure 1.1: Worldwide capacity share of different non-hydro renewable powers..... 4

Figure 1.2: Global cumulative wind power capacities from 2001 to 2020 4

Figure 1.3: Inside of a Wind Turbine 5

Figure 1.4: Typical vertical and horizontal axis wind turbine 7

Figure 1.5: Power coefficients (Cp) vs tip speed ratio (λ) for various wind turbines 8

Figure 1.6: Upwind and downwind structure..... 9

Figure 1.7: Aerodynamic forces and velocities at a rotor blade 10

Figure 1.8: Calculated Cp(λ, β) surface base on real data blade 11

Figure 1.9: Effect for different pitch angles with constant speed operation 12

Figure 1.10: Air Flux on a blade profile "stall"..... 12

Figure 1.11: Wind energy conversion system without power converter interface 14

Figure 1.12: Variable speed configuration with variable rotor resistance..... 15

Figure 1.13: Variable speed configuration with reduced capacity converters 16

Figure 1.14: Variable speed configurations with full capacity converters 17

Figure 2.1: DFIG based wind Energy conversion system scheme 19

Figure 2.2: Active power flows in the DFIG during sub-synchronous operation..... 21

Figure 2.3: Active power flow in the DFIG during super-synchronous operation 22

Figure 2.4: PARK model of DFIG 25

Figure 2.5: Representation of the machine in the two-phase frame 26

Figure 2.6: General principle of vector control in stator active and reactive power 28

Figure 2.7: Control architecture of the wind system 30

Figure 2.8: Principle of the control of the rotor side converter. 30

Figure 2.9: Control of rotor currents 32

Figure 2.10: Control of rotor side converter..... 33

Figure 2.11: Establishment angles processing using a PLL 34

Figure 2.12: Control diagram of the grid side converter ……..……. 34
Figure 2.13: Simulation results of a vector control of the DFIG …….…….……. 36
Figure 3.1: Scheme of a wind turbine……...……... 39
Figure 3.2: Development of power factor of the wind turbine...…….……... 40
Figure 3.3: Block diagram of the turbine model……..…… 42
Figure 3.4: Wind turbine control strategy based on four speed regions……. 42
Figure 3.5: Block diagram of the maximization of extracted power without speed control….. 44
Figure 3.6: Simulation result of a wind energy conversion chain … …… 46
Figure 4.1: MRAS scheme for speed estimation ……...…… 51
Figure 4.2: Scheme of Principle of the MRAS Observer …….. 52
Figure 4.3: Block diagram of sensorless vector control of the DFIG using (MRAS)…….…... 53
Figure 4.4: Simulation for positioning the rotor without sensor by using MRAS observer….. 55
Figure B.1: Block diagram of the stator power control system …...…….. 59
Figure B.2: Block diagram of the rotor current control system …….…….... 60
Figure B.3: Block diagram of the speed control system……...….. 60

List of Tables

Table A.1: Doubly fed induction machine parameters...…… 58

Table A.2: Turbine parameters……...…..…….…….. 58

Table B.1: PI regulators parameters.....…...…….... 61

General Introduction

Nowadays, the human society consumes a huge amount of electricity every year, renewable energy sources are the only way by which the Earth's energy demand can be met without affecting the climatic conditions. Of the available renewable energy sources, wind energy has become one of the most important and promising sources of renewable energy all over the world.

Wind energy is a free, renewable, clean, and non polluting source of electricity. Since earliest recorded history, wind power has been used to move ships, grind grains, and pump water. Wind energy was used to propel boats along the Nile River as early 5000 B.C. Simple windmills were used in china to pump water [2].

All electric generating wind turbines, no matter what size, are comprised of a few basic components: the part that actually rotates in the wind, the electrical generator, a speed control system, and a tower. Some wind machines have fail safe shutdown system so that if part of the machine fails, the shutdown system turns the blades out of the wind or puts brakes. Just like solar electric system, wind powered system can be used in two ways: off grid or on grid is when your home or business is entirely disconnected from electric utility company, and we generate absolutely all of the electricity we need. Usually these systems cost about 30% more than an on-grid (or grid-tie system) [2].

Wind power generation uses either fixed speed or variable speed turbines. Variable speed wind turbine system based on DFIG has become the most popular configuration in wind energy conversion system due to its merits of variable speed constant frequency operation, decoupled active/reactive power control, maximum power capture capability, reduced mechanical stress, low converter VA rating (usually 30% of the generator capacity), and reduced power loss compared to other solutions such as fixed speed induction generators or fully rated converter systems [22].

All of those above mentioned advantages of the DFIG are possible because of the control scheme that can be implemented in the back to back converters of the DFIG. Hence, the method of controlling back to back converter plays a significant role in achieving better performance of the DFIG system. A speed sensor is usually needed for vector control of the DFIG scheme. The use of position encoder has several drawbacks in term of robustness, cost, cabling, and maintenance, so sensorless operation is desirable.

The main goal of our report is to study the sensorless control technique likely to optimise the production of a wind turbine, in particular that using a doubly fed asynchronous generator (DFIG). To do this, the present work is organised as follows:

Chapter one includes an overview about wind energy, the constituent elements and the modeling of the wind turbine.

In the second chapter, a modeling of the DFIG will be presented. This will be followed by the establishment of the control strategy that will allow the machine to have a fixed speed operation. This is possible through the introduction of dual feeding. A constant supply at the stator, another variable voltage and frequency at the rotor. This strategy consists of vector control that allows independent control of the active and reactive powers.

Third chapter that control of the wind system will be presented using the maximum power point tracking (MPPT) strategy is based on principle of extracting the maximum power from the wind turbine and its injection into the network. The vector control of active and reactive power stator allows adjustment of these according to instructions determined in advance by the network manager. The simulation results will be presented with the objective of verifying and validating the strategies of control.

In the fourth chapter, the model reference adaptive system (MRAS) observer used for sensorless control of DFIG. Simulation tests analyse are confirm the good performance and robustness of this control witch proposed in this work.
Finally, we close this thesis with a general conclusion that will bring perspectives for the continuity of this work in the future.

CHAPTER ONE

Basics of Wind Power Generation System

1.1. Introduction

Over the last twenty years, renewable energy sources have been attracting great attention due to the cost increase, limited reserves, and adverse environmental impact of fossil fuels. In the meantime, technological advancements, cost reduction, and governmental incentives have made some renewable energy sources more competitive in the market. Among them, wind energy is one of the fastest growing renewable energy sources [1].

Wind energy has been used for hundreds of years for milling grains, pumping water, and sailing the seas. The use of windmills to generate electricity can be traced back to the late nineteenth century with the development of a 12kW DC windmill generator. It is, however, only since the 1980s that the technology has become sufficiently mature to produce electricity efficiently and reliably. Over the past two decades, a variety of wind power technologies have been developed, which have improved the conversion efficiency and reduced the costs for wind energy production. The size of wind turbines has increased from a few kilowatts to several megawatts each. In addition to onshore installations, larger wind turbines have been pushed to offshore locations to harvest more energy and reduce their impact onshore use and landscape. This chapter provides an overview of wind power generation systems and a background on several aspects related to this stimulating technology [3,4].

1.2. Renewable energy development

Renewable energy is defined as the energy that comes from resources that are naturally replenished on a human timescale such as sunlight, wind, rain, tides, waves and geothermal heat. Typically, the renewable energy includes wind power, photovoltaic (PV) power, hydropower, biomass power, and ocean power. As renewable energy is reproducible and has a low footprint of CO2, it is regarded as a favorable solution to both the global environment challenge and energy crisis. Rapid deployment of renewable energy has been reported in recent years. Global renewable energy policy multi stakeholder network REN21 estimated that by the end of 2016, 30% power generation capacity will come from renewable energy and renewable energy will account for about 24.5% of global electricity generation [3]. Nowadays, the biggest renewable energy generation is from hydropower. However, since the location requirement of the hydropower is limited to lakes or rivers, the worldwide growth of hydropower has become slower in the recent years, which indicates that hydropower is very close to its capacity limit. The non-hydropower renewable generation, including wind, PV, and biomass, has been growing very fast in the last 10 years. The non hydropower renewable generation capacity reached 921 GW by the end of 2016, compared to 85 GW in 2004 [3].

The worldwide capacity share of different non hydro renewable powers by the end of 2016 can be found in Figure 1.1. It is found that wind power has the largest capacity share among the non hydropower renewable generations. Wind power has reached 56.8% of the non-hydro renewable power capacity.

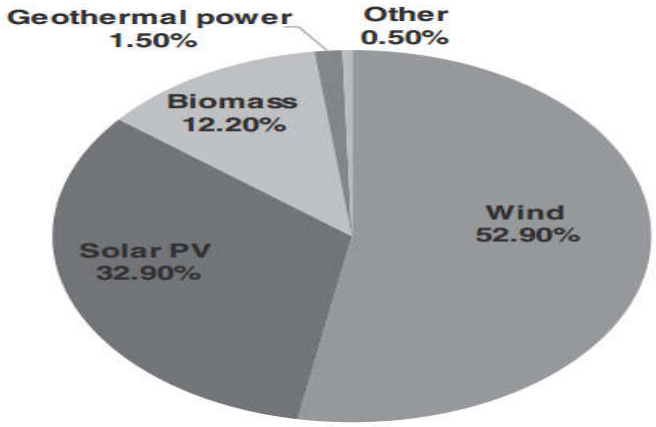

Figure 1.1: Worldwide capacity share of different non hydro renewable powers by the end of 2016 [3].

1.3. Wind energy development

Wind power has truly become an important component of the modern energy supply. The cumulative wind power capacity from 2001 to 2020 is shown in Figure 1.2; the installed capacity of wind power achieved 487 GW, with 54 GW added in 2016 alone. Wind power accounted for 55% of the renewable power capacity globally, not including hydropower, and accounted for 3.7% of global electricity production by the end of 2015 [5, 6].

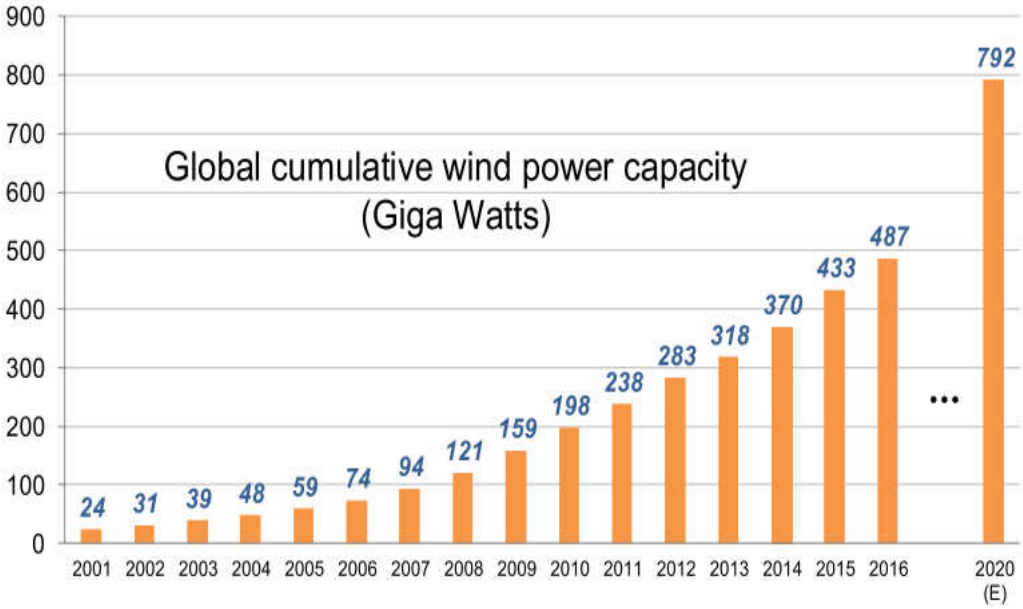

Figure 1.2: Global cumulative wind power capacities from 2001 to 2020 [4].

Today the major wind turbine manufacturers have issued products in the power range of 4–6 MW, and it is expected that more wind turbines above 4 MW will be erected in the next decade (with 10MW prototypes also available); this trend is mainly driven by the need to reduce the cost of energy per produced kilowatt hour [7]. With respect to the wind power markets and manufacturers in 2015, China was the largest market with over 30 GW newly added in 2015, together with the United States (8.6 GW) and the European Union (12.8 GW) sharing approximately 82% of the global market. The companies from China, the United States, and Europe dominated the market shares with wind turbines of 1.5–3.5 MW in the mainstream and 5–8 MW at the high end in terms of power level [5].

1.4. Basic structure of a wind turbine

The mostly used wind turbine is the horizontal wind turbine as shown in figure 1.4. The blade, the shaft and the nacelle of the wind turbine are installed on a high tower. The blade rotates under wind flow and the wind energy is captured and converted into the mechanical energy in the shaft. The rotating angular speed of the shaft is increased using the gearbox so that it is compatible with the generator. The mechanical energy originated from the wind is converted into electric energy by the generator. Then the electricity is transmitted to the power electronic converter on the ground via the power cable, which is connected to the transformer in the grid. The nacelle provides space for components such as the shaft, the gearbox, and the brake on the tower, and can also target the turbine toward the wind flow direction by the action of the yaw.

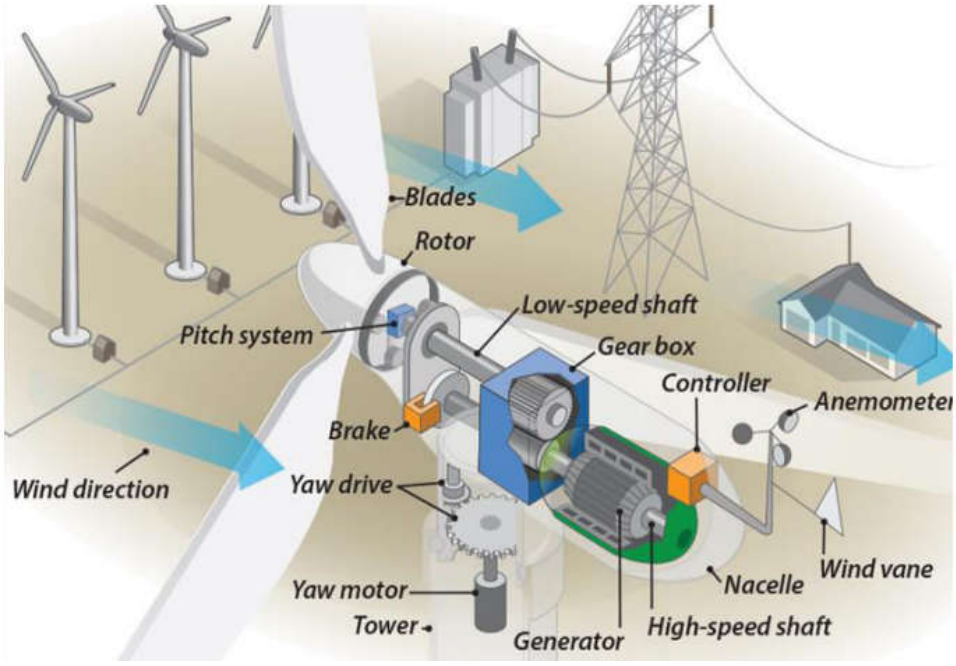

Figure 1.3: Inside of a Wind Turbine [8].

The following are the components of the wind turbine and its functions

Anemometer: Measures the wind speed and transmits wind speed data to the controller.

Blades: Rotates when wind is blown over them, causing the rotor to spin. Most turbines have either two or three blades.

Brake: Stops the rotor mechanically, electrically, or hydraulically, in emergencies.

Controller: Starts up the machine at wind speeds of about 8 to 16 miles per hour (mph) and shuts off the machine at about 55 mph. Turbines do not operate at wind speeds above about 55 mph because they may be damaged by the high winds [8].

Gear box: The main function is to connect the low speed shaft to the high-speed shaft so that the speed is increased from 30-60 rotations per minute (rpm) to about 1000-1800 rpm; the speed which is required by generators to produce electricity [8].

High-speed shaft: Drives the generator.

Low-speed shaft: Rotates the low speed shaft at 30-60 rpm speed.

Nacelle: It contains the gear box, the shafts, generator, controller, and brake [8].

Pitch: The main function of pitch is to adjust the blades of the wind turbine in or out of the wind speed to control the rotor speed so that rotor speed is within the allowed operational limit.

Rotor: Blades and hub together form the rotor.

Wind vane: Measures wind direction and communicates with the yaw drive to orient the turbine properly with respect to the wind.

Yaw drive: Orients upwind turbines to keep them facing the wind when the direction changes. Downwind turbines don't require a yaw drive because the wind manually blows the rotor away from it.

Yaw motor: Powers the yaw drive.

1.5. Classification of wind turbine

Wind turbines are usually classified into two categories, according to the orientation of the axis of rotation with respect to the direction of wind, as shown in Figure 1.5 [9, 10]:

· Vertical-axis turbines

· Horizontal-axis turbine

1.5.1. Vertical axis wind turbine (VAWT)

The first windmills were built based on vertical axis structure. This type has only been incorporated in small scale installations. Typical VAWTs include the Darrius rotor, as shown in figure 1.5 (a).

Advantages of the VAWT [11, 12] are:

· Easy maintenance for ground mounted generator and gearbox,

· Receive wind from any direction (No yaw control required), and

· Simple blade design and low cost of fabrication.

Disadvantages of vertical axis wind turbine are:

· Not self starting, thus, require generator to run in motor mode at start,

· Lower efficiency (the blades lose energy as they turn out of the wind),

· Difficulty in controlling blade over speed, and

· Oscillatory component in the aerodynamic torque is high.

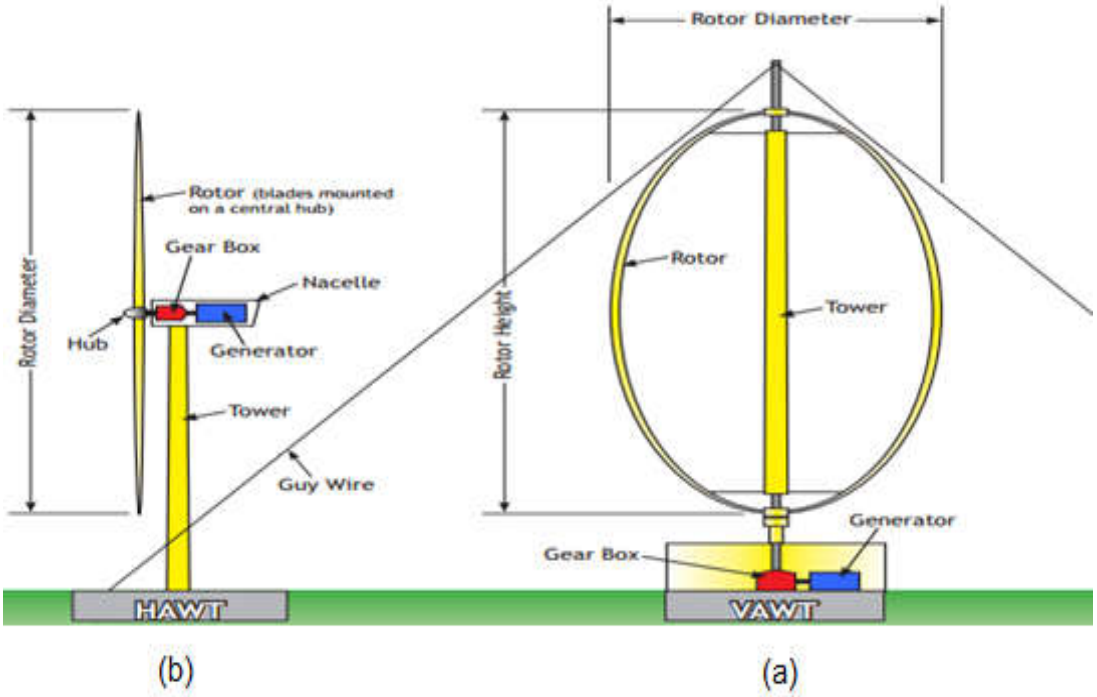

Figure 1.4: (a) a typical vertical-axis turbine (the Darrius rotor) (b) a horizontal-axis wind turbine.

1.5.2. Horizontal-axis wind turbines (HAWT)

The most common design of modern turbines is based on the horizontal-axis structure. Horizontal axis wind turbines are mounted on towers as shown in Figure 1.5 (b). The tower's role is to raise the wind turbine above the ground to intercept stronger winds in order to harness more energy.

Advantages of the HAWT:

· Higher efficiency,

· Ability to turn the blades, and

· Lower cost to power ratio.

Disadvantages of horizontal-axis:

- Generator and gearbox should be mounted on a tower, thus restricting servicing, and
- More complex design required due to the need for yaw or tail drive.

1.5.3. Number of blades

Horizontal axis wind turbines can have different number of blades, depending on the purpose of the turbine. Two bladed or three bladed turbines are usually used for electric power generation due to their higher angular speeds. Turbines with 20 or more blades are used for mechanical water pumping due to their higher mechanical torque. To extract the maximum possible wind power, each blade should interact as much as possible with the wind passing through the swept area. Therefore, a fewer number of blades results in a higher angular speed of the turbine, because the blades have to move faster to fill up the swept area. A wind turbine with a high number of blades has a low angular speed but a high mechanical torque. In contrast, a wind turbine with only two or three blades has a higher angular speed which allows the use of a smaller and lighter gearbox to achieve the required high speed at the driving shaft of the power generator. Currently, three bladed turbines dominate the market for grid connected horizontal axis wind turbines [21].

1.5.4. Betz limit

An important operational characteristic of wind turbines is the Betz limit. It indicates the theoretical maximum possible energy that the turbine can extract from the wind. If turbines were 100% efficient, which is practically impossible, all the airflow energy would be extracted and the flow speed after passing through the turbine would be zero. In 1928, Betz showed that under ideal assumption of uniform rotor disk with infinite number of blades the maximum efficiency of a turbine is 59.3% (Figure 1.6) [13, 14].

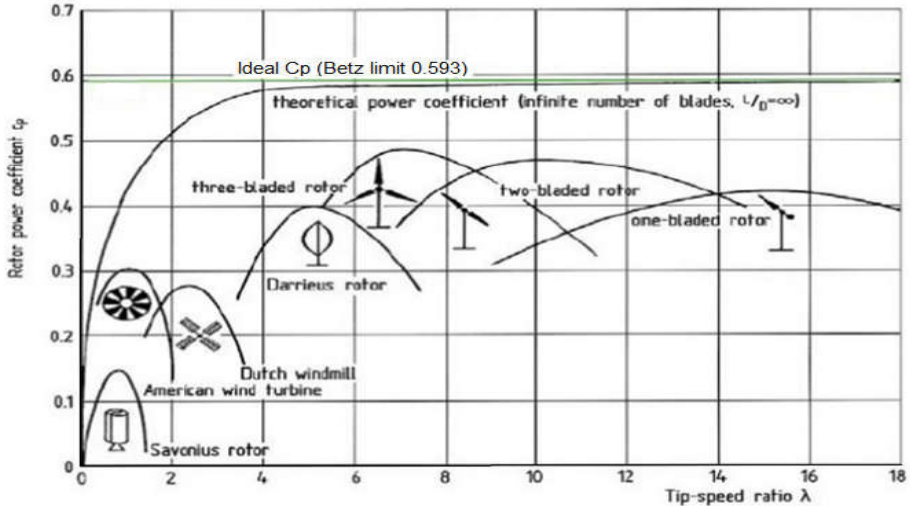

Figure 1.5: Power coefficients (Cp) vs. Tip speed ratio (λ) for various wind turbines.

1.5.5. Upwind and downwind turbines

As shown in Figure 1.7 the upwind configuration, the turbine faces into the wind with the blades in front of the nacelle, whereas a downwind turbine has its blades to the rear of the nacelle and faces away from the wind. An upwind turbine produces a higher power than that in the downwind configuration, because it eliminates the tower shadow on the blades. This results in lower noise, lower blade fatigue, and smoother power output. However, a drawback is that the turbine must constantly be turned into the direction of wind by the yaw mechanism. The heavier yaw mechanism of an upwind turbine requires a heavy duty and stiffer rotor compared to a downwind configuration. In contrast, the downwind turbine has the wind shade of the tower in the front and loses some power from the slight wind drop.

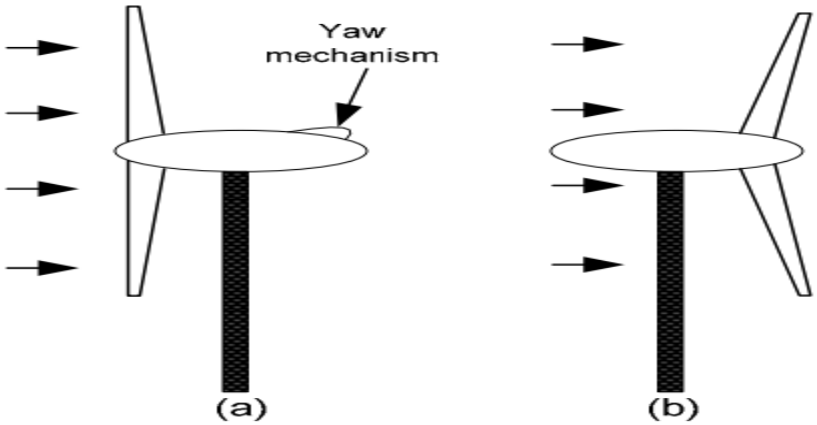

Figure 1.6: (a) Upwind structure (b) Downwind structure [12].

However, it allows the use of a free yaw system. It also allows the blades to deflect away from the tower when loaded. Its drawback is that the turbine may yaw in the same direction for a long period of time, which can twist the cables that carry current from the nacelle. Both types have been used in the past. Although, the upwind turbine configuration has become more common [15].

1.6. Wind energy conversion

In this section, properties of the wind, which are of interest in this report, will be described. First the wind distribution, i.e., the probability of a certain average wind speed, will be presented. The wind distribution can be used to determine the expected value of certain quantities, e.g. produced power. Then different methods to control the aerodynamic power will be described.

1.6.1. Aerodynamic power control

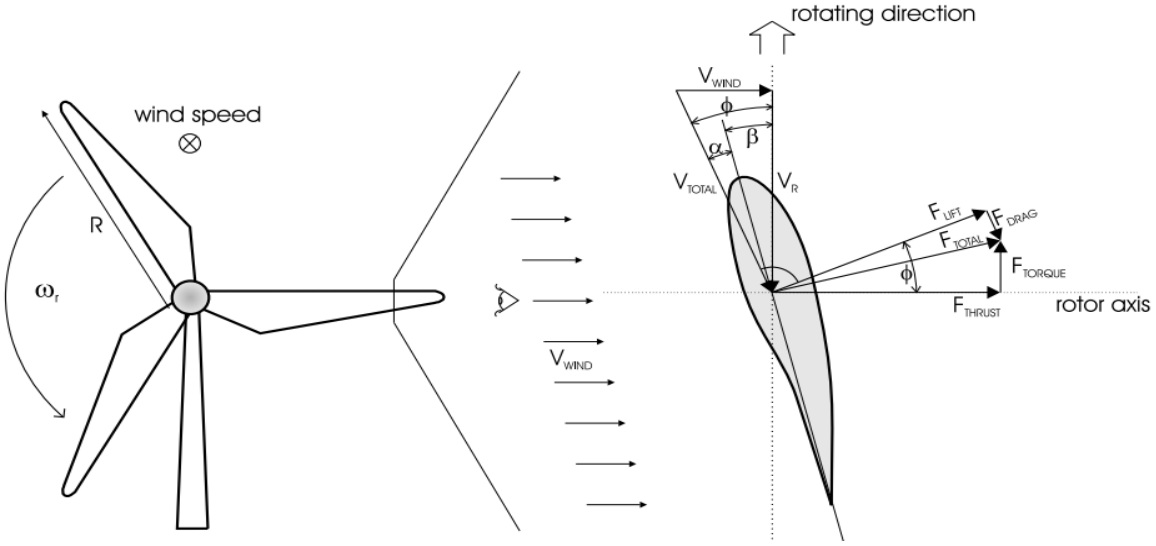

Figure 1.7: Aerodynamic forces and velocities at a rotor blade.

There are two methods to limit the aerodynamic conversion at high wind speed. Pitch control which turn the blades out of the wind and stall control, where the blades lose their aerodynamic efficiency at high wind speeds. The amount of energy that is extracted from wind and converted into mechanical energy is depending on the radial force acting on the blade. The formation of the force depends on particular prof ile design and dimension and is shown in Figure 1.9. The $C_p(\lambda, \beta)$ characteristic gives us a power coefficient, that depends on the tip speed ratio λ and the pitch angle β. For blade profiles two forces are generally used to describe the characteristics, lift force component (F_{lift}) and a drag component (F_{drag}) which resulting as F_{total}. The F_{lift} component and an F_{drag} together are transformed into a pair of axial F_{thrust} force and rotor's directions F_{torque} components, where only the F_{torque} produces the driving torque around the rotor shaft. By varying the pitch angle, β the size the direction of F_{total} components can be changed. The axial forces F_{thrust} has no driving effect but puts stress on rotor blades and furthermore, leads to a thrust on the nacelle and on tower [19].

1.6.1.1. Pitch control

In this method there is a mechanism to physically turn the blades around their longitudinal axes. At low wind speed a control system will use this feature to maximise energy extracted from the wind. During the higher wind speed the torque or power can easily be limited to its rated value by adjusting the pitch angle β. In addition the axial aerodynamics forces are reduced. This method is almost always used with variable speed turbines in order to make operation at high wind speed possible and safety.

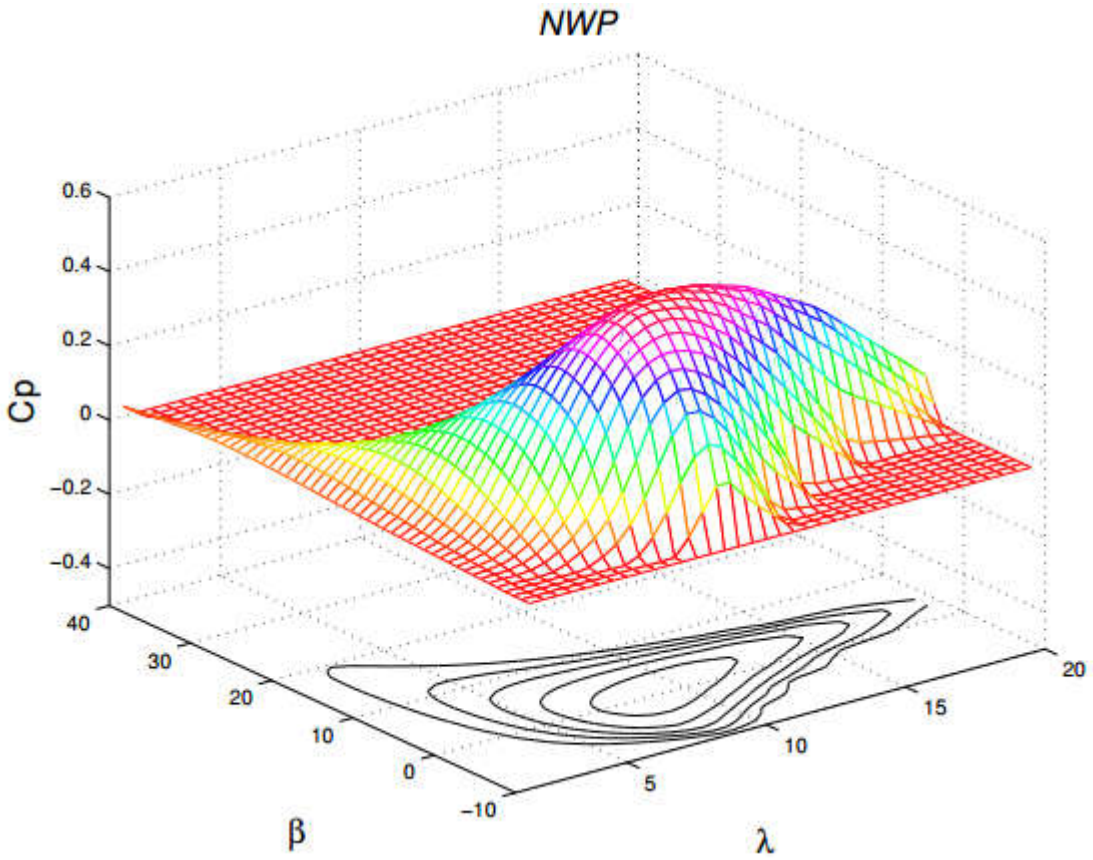

Figure 1.8: Calculated Cp(λ, β) surface base on real data blade[19].

On a pitch controlled wind turbine the turbine´s electronic controller checks the power output of the turbine constantly. When the power output becomes too high, it requested the blade pitch mechanism to immediately turn the blades slightly out of the wind. When the wind speed is less strong the blades are turned back, into the most effective position [19].

1.6.1.2. Passive stall regulation

Passive stall controlled wind turbines have the rotor firmly attached to the hub at a fixed angle. Accordingly, using the passive stall method the pitch angle β is always constant, no mechanism to turn the blades around their axes is necessary. The blades are aerodynamically designed to stall at higher wind speeds, and the incoming power is limited close to the rated. When the wind speed increases, the angle α, which is the angle of attack, will increase. Above a certain angle α, the stall effect occur, the torque producing force can be limited approximately to its rated value. This concept is used for around 60% of the constant speed wind turbine in the world [19].

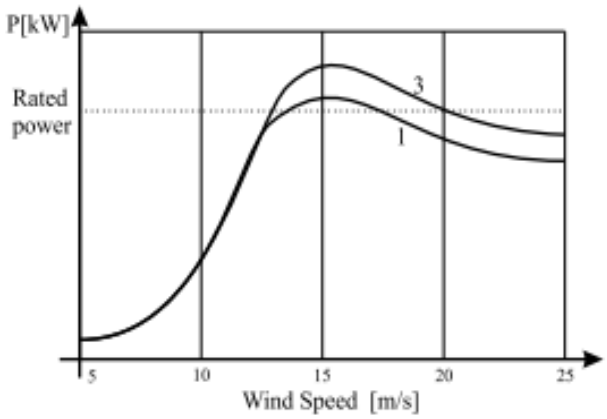

Figure 1.9: Effect for different pitch angles with constant speed operation [19].

Advantages of the stall control system are that moving parts in the rotor blades are avoided and a complex control system is not necessary. On the other hand, stall control involves a very complex aerodynamic design and related design challenges in the structural dynamics of the whole wind turbine, for instance to avoid stall induced vibrations.

A normal passive stall controlled wind turbine usually have a drop in the electrical power output for higher wind speeds, as the rotor blades go into deeper stall, which is a drawback. For fixed speed operation, an advantage is that stall control gives lower power pulsation compared to pitch control [20].

1.6.1.3. Active stall regulation

The active stall regulation offers both, the advantages of pitch controlled blades and the stall effect. Due to the pitch controlled blades, one of the advantages of active stall is that one can control the power output more accurately than with passive stall, so that the average power is always at the rated value at wind speed above rated. As with pitch control it is largely an economic question whether it is worth to pay for the added complexity of the machine, when the blade pitch mechanism is added.

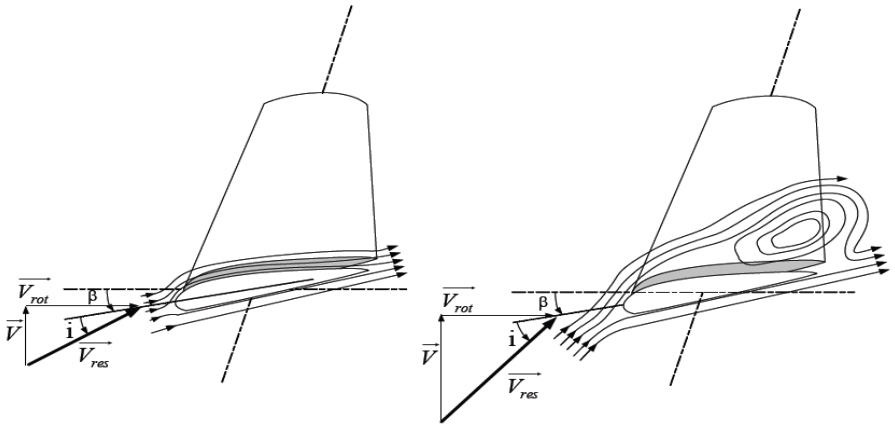

Figure 1.10: Air Flux on a blade profile "stall".

Besides providing power control, the blade pitch system is also used to accelerate the blades from idling to operational speed and bringing the rotor back to a safe idling situation in case of a grid loss or any other functional error.

The rotor blades are able to be pitched like the pitch controlled wind turbines. The difference is that when the machine reaches its rated power, the blades will pitch in the opposite direction, increasing their angle to the wind and going into a deeper stall.

The active stall control system is often installed in the large fixed speed turbines (1 MW and more) [19].

1.7. Wind energy conversion system configurations

The wind turbine is one of the most important elements in wind energy conversion systems. Over the years, different types of wind turbines have been developed [24]. This section provides an overview of wind turbine technologies, including fixed and variable speed turbines.

A fundamental concept in understanding wind technology is wind energy capture. Wind holds in it a discrete amount of power at any given point in time, dependent in large part on the wind speed. As wind speed can vary greatly, wind turbines must be capable of operating over a wide wind speed range. The wind turbine can operate in one of two ways either fixed speed or variable speed. For fixed speed wind turbines, the generator (induction generator) is directly connected to the grid. Since the speed is almost fixed to the grid frequency, and most certainly not controllable, it is not possible to store the turbulence of the wind in form of rotational energy. Therefore, for a fixed-speed system the turbulence of the wind will result in power variations, and thus affect the power quality of the grid [25]. For a variable speed wind turbine the generator is controlled by power electronic equipment, which makes it possible to control the rotor speed. In this way the power fluctuations caused by wind variations can be more or less absorbed by changing the rotor speed [26] and thus power variations originating from the wind conversion and the drive train can be reduced. Hence, the power quality impact caused by the wind turbine can be improved compared to a fixed speed turbine [27].

The generator and power converter in a wind energy conversion system are the two main electrical components. Different designs and combinations of these two components lead to a wide variety of WECS configurations [24], which can be classified into three groups:

(1) Fixed speed WECS without power converter interface,

(2) WECS using reduced capacity converters, and

(3) Full capacity converter operated WECS.

In this section the above wind turbine systems will be presented:

1.7.1. Fixed speed wind turbine

A typical configuration of WECS without a power converter interface is illustrated in Figure 1.15, where the generator is connected to the grid through a transformer. A squirrel cage induction generator (SCIG) is exclusively used in this type of WECS, and its rotational speed is determined by the grid frequency and the number of poles of the stator winding. For a four-pole megawatt generator connected to a grid, the generator operates at a speed slightly higher than 1800 rpm. At different wind speeds, the generator speed varies within 1% of its rated speed. A gearbox is normally required to match the speed difference between the turbine and generator such that the generator can deliver its rated power at the rated wind speed. This configuration requires a soft starter to limit high inrush currents during system start up, but the soft starter is by passed by a switch after the system is started. During normal operation, the system does not need any power converter. A three phase capacitor bank is usually required to compensate for the reactive power drawn by the induction generator.

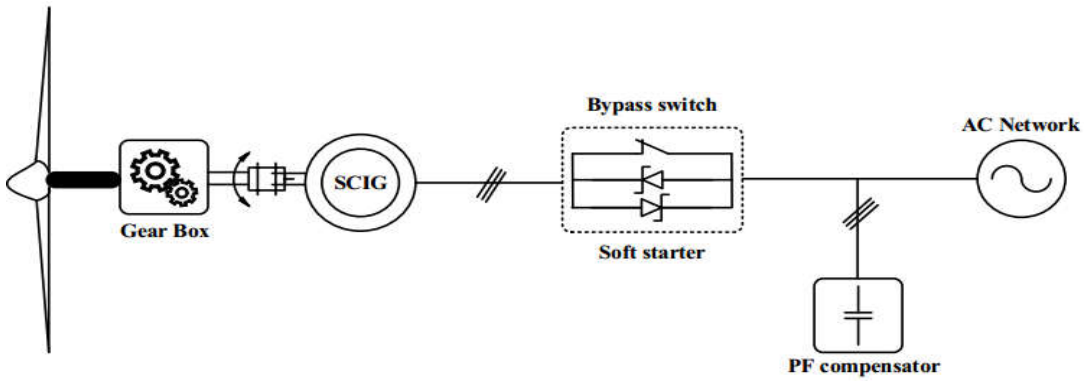

Figure 1.11: Wind energy conversion system without power converter interface.

This wind energy system features simplicity, low manufacturing, maintenance costs, and reliable operation. The main drawbacks include: (1) the system delivers the rated power to the grid only at a given wind speed, leading to low energy conversion efficiency at other wind speeds; and (2) the power delivered to the grid fluctuates with the wind speed, causing disturbances to the grid. Despite its disadvantages, this wind energy system is still widely accepted in industry with a power rating up to a couple of megawatts.

1.7.2. Variable speed wind turbine with reduced capacity converters

Variable speed operation has a series of advantages over fixed speed wind systems. It increases the energy conversion efficiency and reduces mechanical stress caused by wind gusts. The latter has a positive impact on the design of the structure and mechanical parts of the turbine and enables the construction of larger wind turbines. It also reduces the wear and

tear on the gearbox and bearings, expanding the life cycle and reducing the maintenance requirements. The main drawback of variable speed WECS is the need for a power converter interface to control the generator speed, which adds cost and complexity to the system. However, the power converter decouples the generator from the grid, which enables the control of the grid-side active and reactive power [28]. Variable speed WECS can be further divided into two types based on the power rating of the converter with respect to the total power of the system: reduced capacity power converter and full capacity power converter. The variable speed WECS with reduced capacity converters are only feasible with wound rotor induction generators (WRIG) since variable speed operation can be achieved by controlling the rotor currents without the need to process the total power of the system. There are two designs for the WRIG configurations: one with a converter controlled variable resistance, and the other with a four quadrant power converter system.

1.7.2.1. Wound rotor induction generator with variable rotor resistance

Figure 1.16 shows a typical block diagram of the WRIG wind energy system with a variable resistance in the rotor circuit. The change in the rotor resistance affects on the torque and speed characteristics of the generator, enabling variable speed operation of the turbine. The rotor resistance is normally made adjustable by a power converter. The speed adjustment range is typically limited to about 10% above the synchronous speed of the generator [29]. With variable speed operation, the system can capture more power from the wind, but also has energy losses in the rotor resistance. This configuration also requires a soft starter and reactive power compensation. The WRIG with variable rotor resistance has been in the market since the mid 1990s with a power rating up to a couple of megawatts.

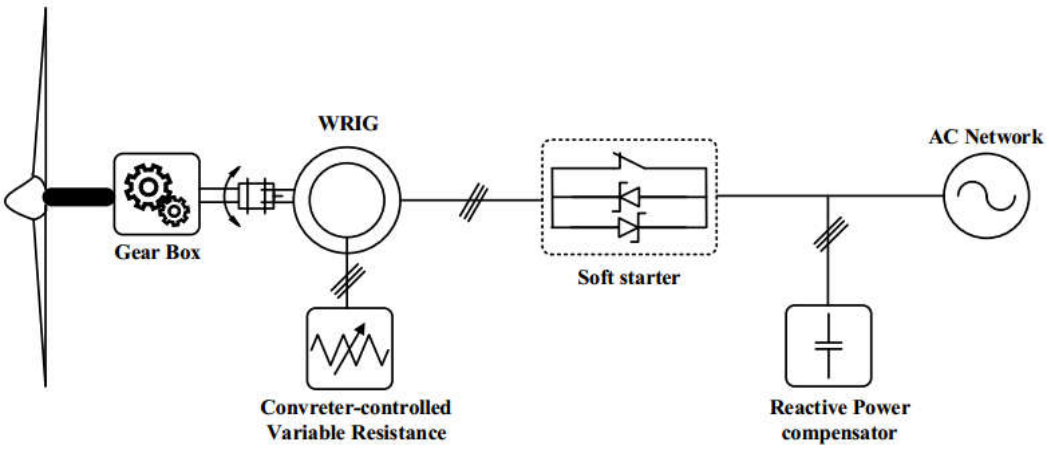

Figure 1.12: Variable speed configuration with variable rotor resistance.

1.7.2.2. Doubly fed induction generator with rotor converter

A typical block diagram of the doubly fed induction generator (DFIG) wind energy system is shown in figure 1.17. The configuration of this system is the same as that of the WRIG system except that (1) the variable resistance in the rotor circuit is replaced by a grid connected power converter system, and (2) there is no need for the soft starter or reactive power compensation. The power factor of the system can be adjusted by the power converters. The converters only have to process the slip power in the rotor circuits, which is approximately 30% of the rated power of the generator, resulting in reduced converter cost in comparison to the wind energy systems using full capacity converters [28].

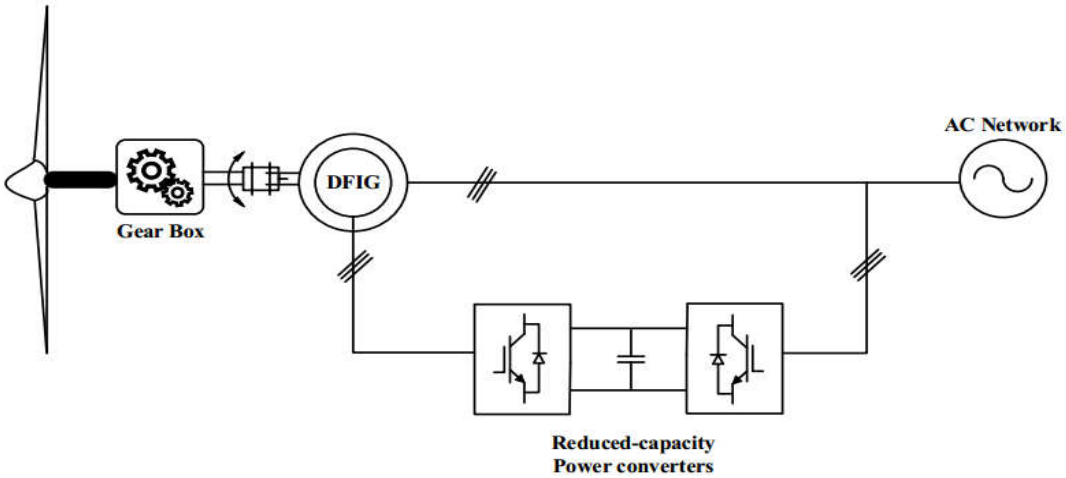

Figure 1.13: Variable speed configuration with reduced capacity converters.

The use of the converters also allows bidirectional power flow in the rotor circuit and increases the speed range of the generator. This system features improved overall power conversion efficiency, extended generator speed range (±30%), and enhanced dynamic performance as compared to the fixed speed WECS and the variable resistance configuration. These features have made the DFIG wind energy system widely accepted in today's market.

1.7.3. Variable speed wind turbine with full capacity power converters

The performance of the wind energy system can be greatly enhanced with the use of a full capacity power converter. Figure 1.18 shows such a system in which the generator is connected to the grid via a full capacity converter system [28]. Squirrel cage induction generators, wound rotor synchronous generators, and permanent magnet synchronous generators (PMSG) have all found applications in this type of configuration with a power rating up to several megawatts. The power rating of the converter is normally the same as that of the generator. With the use of the power converter, the generator is fully decoupled from the grid, and can operate in full speed range.

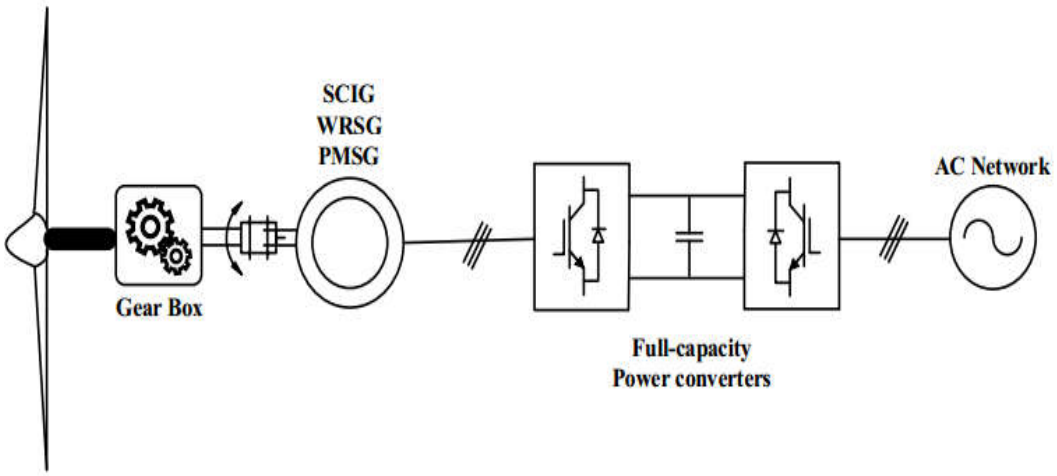

Figure 1.14: Variable speed configurations with full capacity converters.

This also enables the system to perform reactive power compensation and smooth the grid connection. The main drawback is a more complex system with increased costs. It is noted that the wind energy system can operate without the need for a gearbox if a low speed synchronous generator with a large number of poles is used. The elimination of the gearbox improves the efficiency of the system and reduces initial costs and maintenance. However, a low speed generator has a substantially larger diameter to accommodate the large number of poles on the perimeter, which may lead to an increase in generator and installation costs.

1.8. Advantages and disadvantages of wind energy

Let's discuss advantages and disadvantages of wind energy

1.8.1. Advantages of wind energy

- Wind Energy is an inexhaustible source of energy and is virtually a limitless resource.
- Energy is generated without polluting environment.
- This source of energy has tremendous potential to generate energy on large scale.
- Like solar energy and hydropower, wind power taps a natural physical resource.
- Windmill generators don't emit any emissions that can lead to acid rain or greenhouse effect.
- Wind Energy can be used directly as mechanical energy.
- In remote areas, wind turbines can be used as great resource to generate energy.
- In combination with solar energy they can be used to provide reliable as well as steady supply of electricity.

- Land around wind turbines can be used for other uses, e.g. Farming.

1.8.2. Disadvantages of wind energy

- Wind energy requires expensive storage during peak production time.
- It is unreliable energy source as winds are uncertain and unpredictable.
- There is visual and aesthetic impact on region.
- Requires large open areas for setting up wind farms.
- Noise pollution problem is usually associated with wind mills.
- Wind energy can be harnessed only in those areas where wind is strong enough and weather is windy for most parts of the year.
- Usually places, where wind power set up is situated, are away from the places where demand of electricity is there. Transmission from such places increases cost of electricity.
- The average efficiency of wind turbine is very less as compared to fossil fuel power plants. We might require many wind turbines to produce similar impact.
- It can be a threat to wildlife. Birds do get killed or injured when they fly into turbines.
- Maintenance cost of wind turbines is high as they have mechanical parts which undergo wear and tear over the time.

Even though there are advantages of wind energy, the limitations make it extremely difficult for it to be harnessed and prove to be a setback [30].

1.9. Conclusion

This chapter provided an overview of wind energy conversion systems. The basic concepts of wind power, aerodynamic conversion, aerodynamic control, facts, current state, and market trends of wind power technology were presented. The fundamentals of wind energy systems were discussed, including fixed and variable speed operations which complement the in depth analysis of wind energy systems covered in the other chapters of this report.

CHAPTER TWO

Modeling and Vector Control of DFIG

2.1. Introduction

This chapter has the objective to put in evidence the doubly fed induction machine, in order to study its principle of working and the value of advantages and performances brought by this machine, as well as the different domains of application.

In addition, to present the modeling of DFIG, this modeling was based on the development of equivalent diagrams drifted of the theory of the rotating field. The simplicity of conception and maintenance of this machine to the favor of the industries, come however with a big physical complexity, as well as the vector control.

2.2. Components of DFIG

DFIG, as mentioned earlier, is basically a conventional wound rotor induction machine in which the stator is directly connected to the grid through a transformer, and the connection of the rotor to the stator (and grid) is via a back to back voltage source convertor. The rotor converter system consists of a grid side converter (GSC) and rotor side converter (RSC) connected via a DC link. A simplified schematic diagram of a DFIG based wind energy generation system is shown in figure 2.1.

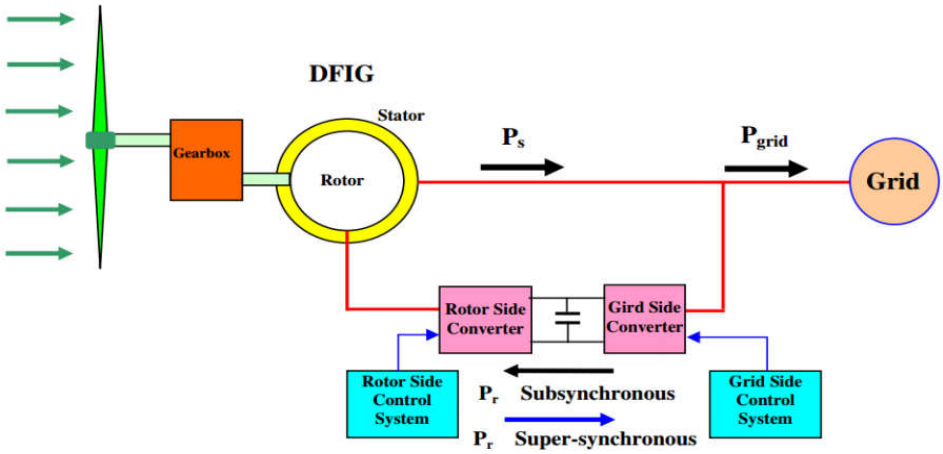

Figure 2.1: DFIG based wind Energy conversion system scheme.

The generator is called DFIG because the power is fed from both stator and the rotor circuits to the grid. The rotor circuit handles typically about 25-30% of the generator rated power, this percentage allows the DFIG to have about ±30% operational speed range around the synchronous speed and reduces the rating and the cost of the rotor converter [31, 32]. The size of the converter is not related to the total generator power but to the selected speed range and, hence, to the "slip" power, thus the cost of the converter increases when the speed range becomes wider. The selection of the speed range, therefore, is based on the economic optimisation of investment costs and on increased efficiency. Since the DFIG is connected to the grid, the high transient currents due to the grid disturbances may destroy the power

electronic devices of the rotor converter. A protection system called "crowbars" are being used in which the rotor winding can be short circuited during the fault period via a small resistance and released when the fault is cleared.

2.3. Principle of Operation of DFIG

Large doubly fed electric machines in the industry are three phase wound rotor type. Although their principles of operation have been known for decades, the massive application has only recently entered and is almost exclusively due to the advent of wind power technologies. The DFIG operates in both sub-synchronous (rotor speed lower than synchronous speed) and super-synchronous (rotor speed higher than synchronous speed) modes which allows an operational speed range of about ±30% around the synchronous speed.

The main advantage of doubly fed induction generator when used in wind turbines is that it has the ability to maintain the amplitude and the frequency of the output voltage essentially constant at grid values, no matter the speed of the wind turbine rotor. Because of this, doubly fed induction generator can be directly connected to the AC power network and remain synchronised at all times. Other advantages include the ability to control reactive power from the rotor circuits to the grid, which enables the DFIG to support the voltage stability and power factor correction at the point of common coupling (PCC).

The feature of controlling the rotor speed to overcome the wind speed variation is done by adjusting the frequency of the AC voltages and currents fed to the rotor windings. This principle can be understood by explaining the sub-synchronous and super-synchronous modes of operation discussed below.

2.3.1. Sub-synchronous mode of operation

When the rotor speed of the generator n_{rotor} is below the synchronous speed n_s the rotor frequency f_{rotor} of the voltage induced increases accordingly and (according to the normal convention) is of positive polarity. This positive polarity means that the phase sequence of the AC currents injected into the generator rotor windings will make the rotor magnetic field rotate in the same direction as the generator rotor, and as a result of controlling the phase sequence of injected current the rotor "receives" power from the grid through the rotor converters (GSC and RSC). This approach to control the power flow in the rotor winding of DFIG in the sub-synchronous mode can be explained by understanding the power flow equations of an induction machine, as explained below [33, 34].

P_g is the air gap power, P_m is the mechanical power transferred between the rotor and the shaft, and P_r is the "slip" power (sP_g) that is transferred between the rotor converters and the electrical grid in the case of DFIG. The slip "s" is defined by:

$$s = \frac{\omega_s - \omega_r}{\omega_s} \tag{2-1}$$

The conventional induction motor with short circuited rotor windings runs at a speed lower than its synchronous speed. The mechanical power P_m is considered positive when transferred from the rotor to the shaft and then driving the mechanical load (like pump or fan). In this case the slip is positive ($0 < s < 1$), the air gap power that is transferred from the stator to the rotor will be positive. If the direction of flow for both P_g and P_m is reversed (i.e. P_g and P_m have negative values) the machine will operate in the generator mode (DFIG in sub-synchronous mode). The slip power P_r will also be negative and will be supplied by the converters (RSC and GSC) to the rotor in which the rotor-side converter (RSC) operates as an inverter and the grid side converter (GSC) as a rectifier. The reversion of the slip power direction in the rotor circuit is done by reversing the phase sequence of the AC voltage or current that is injected into the rotor winding of the DFIG. Figure 2.2 shows the slip power flow directions of the DFIG in both sub-synchronous (grid to rotor) and super-synchronous (rotor to grid) modes.

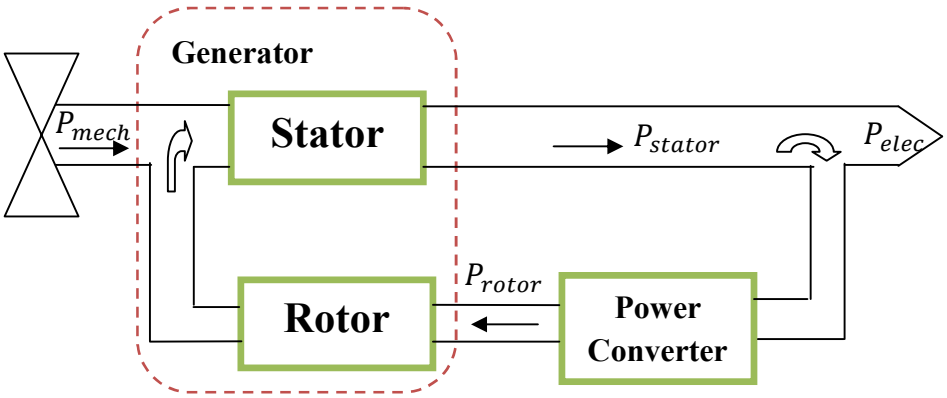

Figure 2.2: Active power flows in the DFIG during sub-synchronous operation.

2.3.2. Super-synchronous mode of operation

Similarly, when the generator rotor speed n_{rotor} increases above the synchronous speed n_s, the frequency f_{rotor} of the ac currents that need to be fed into the generator rotor windings increases accordingly and is of negative polarity now.

The negative polarity of the frequency f_{rotor} indicates that the phase sequence of the three phase AC currents fed into the rotor windings must make the rotor magnetic field rotate in the direction opposite to that of the generator rotor. This means that above the synchronous speed the slip (s) is negative (s < 0), the DFIG operates in the super-synchronous mode, where the slip power Pr is controlled by controlling the phase sequence of the injected currents to the rotor windings of the DFIG. In this mode, the slip power will be positive and transferred from the generator rotor to the grid through the rotor converters of the DFIG, where the RSC operates as a rectifier and the GSC as an inverter.

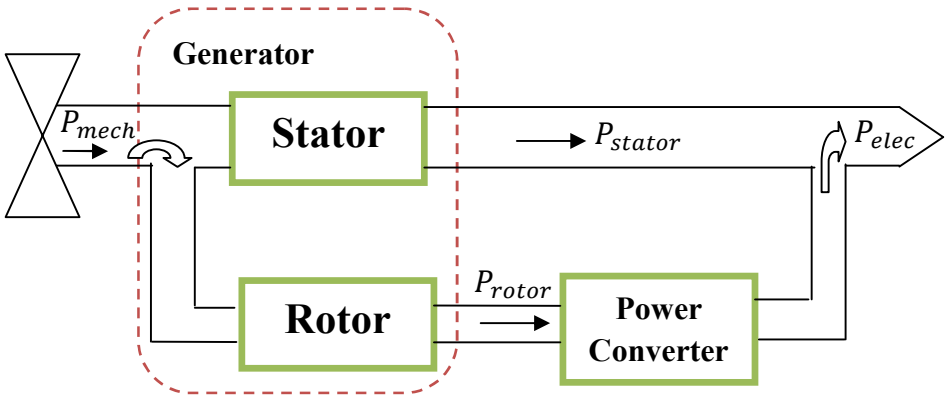

Figure 2.3: Active power flow in the DFIG during super-synchronous operation.

2.4. Advantages and disadvantages of the DFIG

We introduce in this paragraph some of the advantages and the drawbacks of DFIG

2.4.1. Advantages of the DFIG

The DFIG is having lot of advantages than the other types such as FSIG, VSIG and PMSG. Some of the advantages of DFIG are given below.

- It has the ability of decoupling the control of the active and reactive power by controlling the rotor terminal voltages. Hence, the power factor control can be implemented in this system.
- The DFIG is usually a wound rotor induction generator, which is simple in construction and cheaper than a PMSG.
- In a DFIG based wind turbine generator system, the power rating of the power converters is typically rated ±30% around the rated power. This characteristic leads to many merits, such as reduced converter cost, reduced filter volume and cost, less switching losses, less harmonic injections into the connected grid. Improved overall

efficiency (approx. 2-3% more than full scale frequency converter) if only the generator and power converters are considered.

- Aerodynamic, gearbox and converter losses of the DFIG are less.

2.4.2. Disadvantages of the DFIG

The major drawbacks of DFIG are specified below:

- Needs slip rings also it requires frequent maintenance.
- Has limited fault ride through capability and needs protection schemes.
- Have complex control schemes.

2.5. Modeling of DFIG

The modeling of electrical machines consists in the elaboration of mathematical models which make it possible to predict the behavior of the machine in different operating modes, thus anticipating the points which are likely to cause disturbances.

2.5.1. Simplifying assumptions

The asynchronous machine comprises a winding distribution and a very complex geometry. Therefore, for analysis taking into account its exact configuration, the following assumptions have been made for this detailed model [35]:

- The machine is symmetrical,
- The skin effect is neglected,
- Iron losses are neglected,
- Magnetic saturation is neglected.

2.5.2. Mathematical model of doubly fed induction generator

2.5.2.1. Electrical equation of DFIG

In the preceding conditions the equations in matrix form are written:

- For the stator:

$$\begin{bmatrix} V_{as} \\ V_{bs} \\ V_{cs} \end{bmatrix} = \frac{d}{dt}\begin{bmatrix} \psi_{as} \\ \psi_{bs} \\ \psi_{cs} \end{bmatrix} + \begin{bmatrix} R_s & 0 & 0 \\ 0 & R_s & 0 \\ 0 & 0 & R_s \end{bmatrix}\begin{bmatrix} I_{as} \\ I_{bs} \\ I_{cs} \end{bmatrix} \tag{2-2}$$

- For the rotor:

$$\begin{bmatrix} V_{ar} \\ V_{br} \\ V_{cr} \end{bmatrix} = \frac{d}{dt}\begin{bmatrix} \psi_{ar} \\ \psi_{br} \\ \psi_{cr} \end{bmatrix} + \begin{bmatrix} R_r & 0 & 0 \\ 0 & R_r & 0 \\ 0 & 0 & R_r \end{bmatrix}\begin{bmatrix} I_{ar} \\ I_{br} \\ I_{cr} \end{bmatrix} \quad (2\text{-}3)$$

2.5.2.2. Magnetic equations

The stator and rotor fluxes equations in matrix form are given by the following expressions:

$$[\psi_s] = [L_{ss}][i_s] + [M_{sr}][i_r] \quad (2\text{-}4)$$

$$[\psi_r] = [L_{rr}][i_r] + [M_{sr}][i_s] \quad (2\text{-}5)$$

Where: $[L_{ss}] = \begin{bmatrix} l_s & M_s & M_s \\ M_s & l_s & M_s \\ M_s & M_s & l_s \end{bmatrix}$ $[L_{rr}] = \begin{bmatrix} l_r & M_r & M_r \\ M_r & l_r & M_r \\ M_r & M_r & l_r \end{bmatrix}$

And

$$[M_{sr}] = [M_{sr}]^t = M\begin{bmatrix} \cos\theta & \cos(\theta - \frac{2\pi}{3}) & \cos(\theta - \frac{4\pi}{3}) \\ \cos(\theta - \frac{2\pi}{3}) & \cos\theta & \cos(\theta - \frac{4\pi}{3}) \\ \cos(\theta - \frac{4\pi}{3}) & \cos(\theta - \frac{2\pi}{3}) & \cos\theta \end{bmatrix}$$

Where M represents the maximum value of the Stator-Rotor mutual inductance coefficients obtained when the windings are opposite one another.

By replacing relations (2-4) and (2-5) respectively in relations (2-2) and (2-3), we obtain the following two expressions:

$$[V_s] = [R_s][i_s] + [L_{ss}]\frac{d}{dt}[i_s] + \frac{d}{dt}([M_{sr}][i_r]) \quad (2\text{-}6)$$

$$[V_r] = [R_r][i_r] + [L_{rr}]\frac{d}{dt}[i_r] + \frac{d}{dt}([M_{sr}]^t.[i_s]) \quad (2\text{-}7)$$

Where:

$$[V_s] = \begin{bmatrix} V_{sa} \\ V_{sb} \\ V_{sc} \end{bmatrix};\ [V_r] = \begin{bmatrix} V_{ra} \\ V_{rb} \\ V_{rc} \end{bmatrix};\ [i_s] = \begin{bmatrix} i_{sa} \\ i_{sb} \\ i_{sc} \end{bmatrix};\ [i_r] = \begin{bmatrix} i_{ra} \\ i_{rb} \\ i_{rc} \end{bmatrix};\ [\psi_s] = \begin{bmatrix} \psi_{sa} \\ \psi_{sb} \\ \psi_{sc} \end{bmatrix};\ [\psi_r] = \begin{bmatrix} \psi_{ra} \\ \psi_{rb} \\ \psi_{rc} \end{bmatrix}$$

$$[R_s] = \begin{bmatrix} R_s & 0 & 0 \\ 0 & R_s & 0 \\ 0 & 0 & R_s \end{bmatrix};\quad [R_r] = \begin{bmatrix} R_r & 0 & 0 \\ 0 & R_r & 0 \\ 0 & 0 & R_r \end{bmatrix}$$

2.5.2.3. Mechanical equation

The mechanical equation of the machine is described in the form:

$$J\frac{d}{dt}\Omega = T_e - T_r - f.\Omega \qquad (2\text{-}8)$$

This equation leads to differential equations with variable coefficients (2-6) and (2-7). Also the analytical study of the behavior of the system is relatively laborious considering the large number of variables. Then mathematical transformations are used to describe the behavior of the machine using differential equations with constant coefficients.

2.5.3. Doubly fed induction generator model (d-q Model)

The d-q dynamic model of DFIG would be very beneficial in terms of studying the behavior under sub-synchronous and super-synchronous modes of operation and applying the vector control approach to control the output active and reactive power. This model is used to implement vector control in order to control the output active power of the DFIG [36].

2.5.3.1. Park transformation

The transformations is used to convert the three phase magnitudes into two phase magnitudes and is performed in the stationary frame, Figure 2.4 representing the quantity in another reference frame, by projecting the vector on the two orthogonal axes of the new frame, where the d-axis of the excitation frame is aligned with the stator flux.

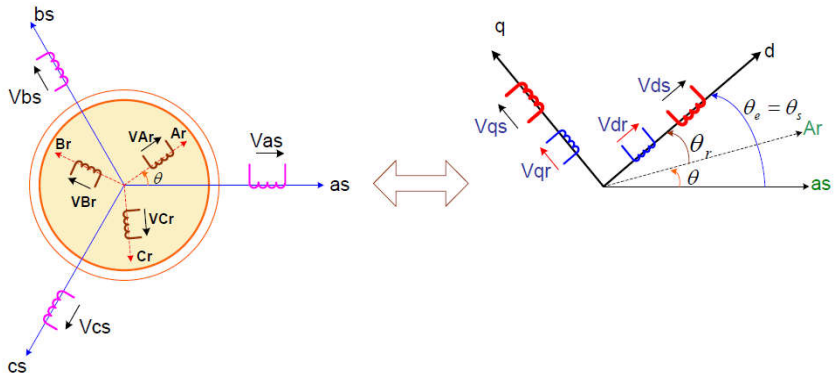

Figure 2.4: PARK model of DFIG.

The asynchronous machine is a strong coupled machine, therefore its representation in the three phase system is particularly complex. For better behavior of an asynchronous machine, it is necessary to use a precise and sufficiently simple model. Then the two axis d-q model given by the Park transformation is used. The new model is obtained by multiplying the

equations of fluxes and tensions by the Park matrix which is expressed by [38]:

$$[P(\theta)] = \sqrt{\frac{2}{3}}\begin{bmatrix} cos\theta & \cos(\theta - {}^{2\pi}/_{3}) & \cos(\theta - {}^{4\pi}/_{3}) \\ -sin\theta & -\sin(\theta - {}^{2\pi}/_{3}) & -\sin(\theta - {}^{4\pi}/_{3}) \\ \frac{1}{\sqrt{2}} & \frac{1}{\sqrt{2}} & \frac{1}{\sqrt{2}} \end{bmatrix} \quad (2\text{-}9)$$

It is noted in figure 2.5 that θs and θr are the angle of the Park transformation of stator and rotor magnitudes respectively.

The transformation of Park leads to a relation linking the angles θs and θr, which expresses by:

$$\theta + \theta_r = \theta_s$$

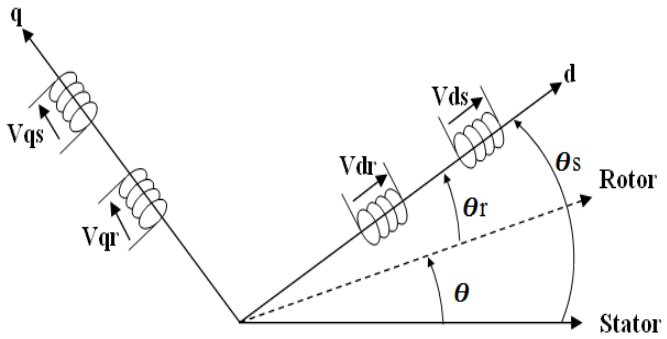

Figure 2.5: Representation of the machine in the two-phase frame.

2.5.3.2. Voltages equation

We apply Park's transformation to expression (2-2) and multiplying the two members of equality by $[P(\theta_s)]$ and simplifying, we will have:

$$[V_{sdq}] = [R_s][i_{sdq}] + \frac{d}{dt}[\psi_{sdq}] + [P(\theta_s)]\frac{d}{dt}[P^{-1}(\theta_s)][\psi_{sdq}] \quad (2\text{-}10)$$

Then the expression (2-10) becomes:

$$\begin{bmatrix} V_{ds} \\ V_{qs} \end{bmatrix} = \begin{bmatrix} R_s & 0 \\ 0 & R_s \end{bmatrix}\begin{bmatrix} i_{ds} \\ i_{qs} \end{bmatrix} + \frac{d}{dt}\begin{bmatrix} \psi_{ds} \\ \psi_{qs} \end{bmatrix} + \begin{bmatrix} 0 & \frac{d\theta_s}{dt} \\ \frac{d\theta_s}{dt} & 0 \end{bmatrix}\begin{bmatrix} \psi_{ds} \\ \psi_{qs} \end{bmatrix} \quad (2\text{-}11)$$

Similarly, by the same steps we obtain the rotor expression as the following:

$$\begin{bmatrix} V_{dr} \\ V_{qr} \end{bmatrix} = \begin{bmatrix} R_r & 0 \\ 0 & R_r \end{bmatrix}\begin{bmatrix} i_{dr} \\ i_{qr} \end{bmatrix} + \frac{d}{dt}\begin{bmatrix} \psi_{dr} \\ \psi_{qr} \end{bmatrix} + \begin{bmatrix} 0 & \frac{d\theta_r}{dt} \\ \frac{d\theta_r}{dt} & 0 \end{bmatrix}\begin{bmatrix} \psi_{dr} \\ \psi_{qr} \end{bmatrix} \quad (2\text{-}12)$$

We write:

$$\begin{cases} [V_{ds}] = [R_s][i_{ds}] + \dfrac{d}{dt}[\psi_{ds}] - \omega_s \psi_{qs} \\ [V_{qs}] = [R_s][i_{qs}] + \dfrac{d}{dt}[\psi_{qs}] + \omega_s \psi_{ds} \end{cases} \quad (2\text{-}13)$$

By analogy, the following voltages are obtained for the rotor quantities:

$$\begin{cases} [V_{dr}] = [R_r][i_{dr}] + \dfrac{d}{dt}[\psi_{dr}] - (\omega_s - \omega)\psi_{qr} \\ [V_{qr}] = [R_r][i_{qr}] + \dfrac{d}{dt}[\psi_{qr}] + (\omega_s - \omega)\psi_{dr} \end{cases} \quad (2\text{-}14)$$

With:

$$\frac{d\theta_s}{dt} = \omega_s ; \frac{d\theta_r}{dt} = \omega_s - \omega = s\omega_s = \omega_r$$

2.5.3.3. Flux equation

The flux matrix system is written in the following form:

- For the stator:

$$\begin{bmatrix} \psi_{ds} \\ \psi_{qs} \end{bmatrix} = \begin{bmatrix} L_s & 0 \\ 0 & L_s \end{bmatrix} \begin{bmatrix} i_{ds} \\ i_{qs} \end{bmatrix} + \begin{bmatrix} L_m & 0 \\ 0 & L_m \end{bmatrix} \begin{bmatrix} i_{dr} \\ i_{qr} \end{bmatrix} \quad (2\text{-}15)$$

- For the rotor:

$$\begin{bmatrix} \psi_{dr} \\ \psi_{qr} \end{bmatrix} = \begin{bmatrix} L_r & 0 \\ 0 & L_r \end{bmatrix} \begin{bmatrix} i_{dr} \\ i_{qr} \end{bmatrix} + \begin{bmatrix} L_m & 0 \\ 0 & L_m \end{bmatrix} \begin{bmatrix} i_{ds} \\ i_{qs} \end{bmatrix} \quad (2\text{-}16)$$

Where the cyclic inductances:

$$L_s = l_s - M_{sr} ; L_m = \frac{3}{2} M_{sr} \text{ and } L_r = l_r - M_{rs}$$

2.5.3.4. Electromagnetic torque equation

After the change of variable, the expression of the electromagnetic torque can be expressed in different forms, one finds this one [38]:

$$T_e = p(\psi_{ds} i_{qs} - \psi_{qs} i_{ds}) \quad (2\text{-}17)$$

$$T_e = p.M(i_{qs}.i_{dr} - i_{ds}.i_{qr}) \quad (2\text{-}18)$$

$$T_e = \frac{p.M}{L_r}(\psi_{dr}.i_{qs} - \psi_{qr}.i_{ds}) \quad (2\text{-}19)$$

$$T_e = \frac{p.M}{L_s}(\psi_{qs}.i_{dr} - \psi_{ds}.i_{qr}) \quad (2\text{-}20)$$

2.5.3.5. Active and reactive power equations

The active and reactive power of the stator and rotor are written as follows [38, 39]:

$$\begin{cases} P_s = V_{ds} I_{ds} + V_{qs} I_{qs} \\ Q_s = V_{qs} I_{ds} - V_{ds} I_{qs} \end{cases} \quad (2\text{-}21)$$

$$\begin{cases} P_r = V_{ds} I_{ds} + V_{qs} I_{qs} \\ Q_r = V_{qs} I_{ds} - V_{ds} I_{qs} \end{cases} \quad (2\text{-}22)$$

2.6. Fundamentals of vector control of induction machines

A vector controlled induction machine operates very similarly like a separately excited DC machine in which the flux and torque can be controlled independently by the field current (Ia) and the armature current (If) respectively. In the case of a DC machine the electro-magnetic (developed) torque is given as a function of both armature and field currents as:

$$T_e = K I_a I_f \quad (2\text{-}23)$$

Where, I_a and I_f are the armature and the field currents, respectively. The armature current produces the armature flux ψ_a (in phase) which is perpendicular to the field flux ψ_f produced by the field current I_f. The electromagnetic torque of a vector-controlled induction machine can be expressed as a function of both i_{ds} and i_{qs} as following.

$$T_e = K . i_{ds} . i_{qs} \quad (2\text{-}24)$$

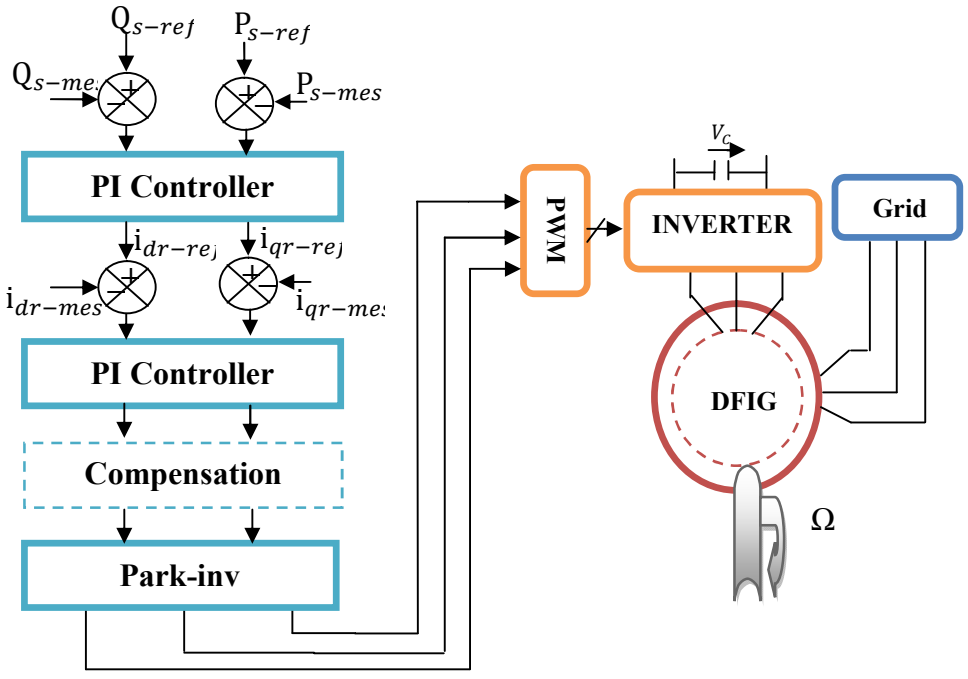

Figure 2.6: General principle of vector control in stator active and reactive power.

Vector control is one of the most common methods applied to DFIG to control the flow of active and reactive power between the stator and the grid. It can be applied on both rotor side converter (RSC) and grid side converter (GSC). [37].

2.7. Vector control of doubly fed induction generator

DFIG control strategies are based on two different approaches [37]:

- Flow control in closed loop, where the frequency and voltage are considered variables (unstable grid).
- Flow control in open loop when the voltage and frequency are constant (stable grid).

In our study, the frequency and voltage are deemed to be unchanging. We can be clear from equation (2-18), the strong coupling between flux and currents. Indeed, the electromagnetic torque is the cross product between flux and stator currents, making the control of DFIG particularly difficult. To simplify ordering, we approximate the model to that of the DC machine which has the merit of having a natural coupling between flux and currents. For this, we apply vector control, also known order by the direction of flow. We choose (d-q) reference linked to the rotating field figure 2.6.

2.7.1. Stator field oriented of the DFIG

The control strategy, using the model of DFIG in (d-q) reference with the vector stator flux aligned with d-axis [44, 45, 46, 51]:

Simplified expression of the electromagnetic torque is obtained by setting the following conditions:

$$\begin{cases} \psi_{qs} = \dfrac{d\psi_{qs}}{dt} = 0 \\ \psi_{ds} = \psi_{s} \end{cases} \tag{2-25}$$

The voltage equations and the flux equations of the stator can be simplified in steady state as:

$$\begin{cases} V_{ds} = 0 \\ V_{qs} = V_{s} = \omega_{s}\psi_{s} \end{cases} \tag{2-26}$$

$$\begin{cases} \psi_{s} = L_{s} i_{ds} + M i_{dr} \\ 0 = L_{s} i_{qs} + M i_{qr} \end{cases} \tag{2-27}$$

The architecture of the controller is illustrated in figure 2.8. It is built on the three phase model of the electromechanical conversion chain of the wind energy system [41].

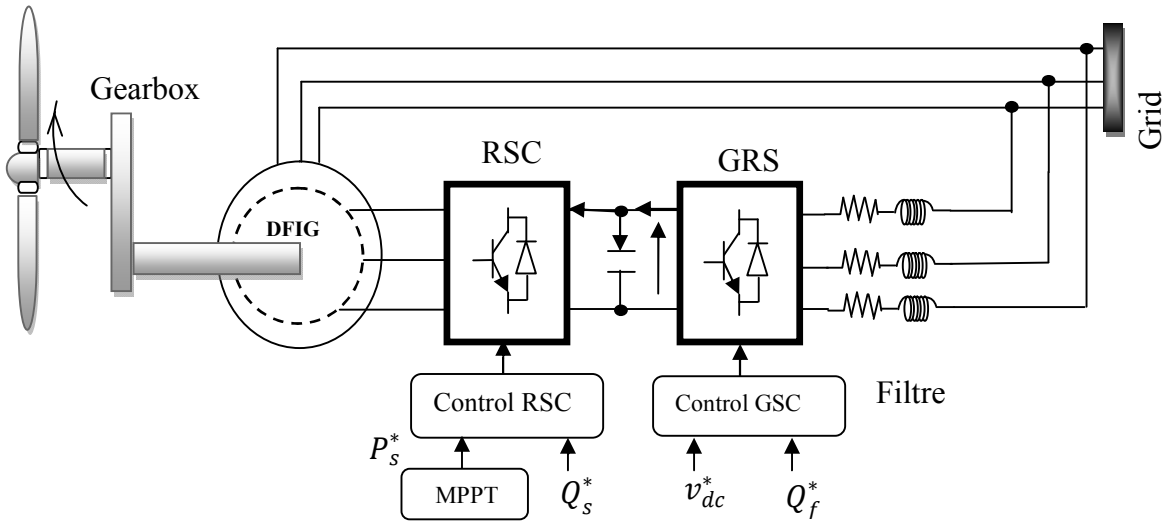

Figure 2.7: Control architecture of the wind system.

Three commands are needed:

- Maximum extraction control wind power by controlling said MPPT (detailed in next chapter).
- Control of RSC by controlling the electromagnetic torque and stator reactive power of DFIG.
- Control of GSC by controlling the voltage of the DC bus and the active and reactive power exchanged with the grid.

2.7.2. Control of the rotor side converter (RSC)

The principle of the control of the rotor side converter is shown in figure 2.9[41].

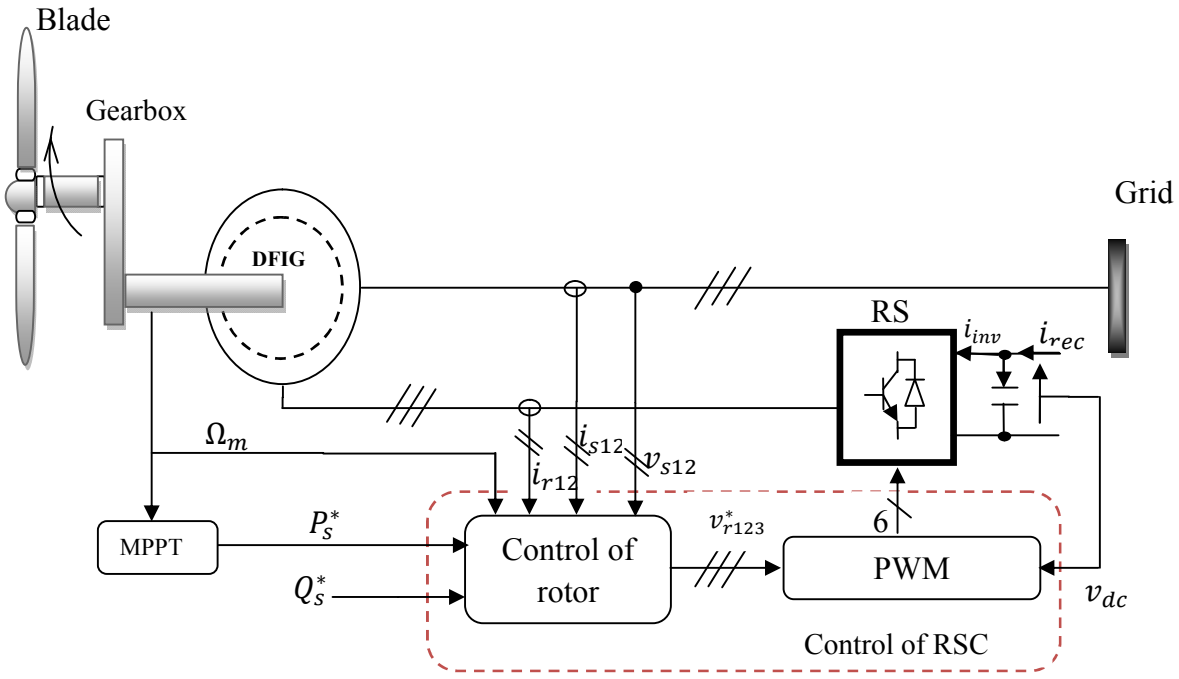

Figure 2.8: Principle of the Control of the rotor side converter.

2.7.2.1. Relation between stator and rotor current

The controls of electromagnetic torque and stator reactive power will be obtained by controlling the rotor (dq) axes currents of DFIG. From the equations (26) to (27) we obtain the expression of the stator current:

$$\begin{cases} I_{ds} = \dfrac{\psi_s}{L_s} - \dfrac{M}{L_s} i_{dr} \\ I_{qs} = -\dfrac{M}{L_s} i_{qr} \end{cases} \tag{2-28}$$

2.7.2.2. Expression of rotor voltage with function of rotor current

By substituting the previous and the equations (2-17) of the rotor flux which then becomes:

$$\begin{cases} \psi_{dr} = \sigma \cdot L_r \cdot i_{dr} + \dfrac{MV_s}{\omega_s L_s} \\ \psi_{qr} = \sigma \cdot L_r \cdot i_{qr} \end{cases} \tag{2-29}$$

With: $\sigma = \left(1 - \dfrac{M^2}{L_r \cdot L_s}\right)$; the dispersion coefficient of the DFIG.

Substituting the expressions of the direct and quadrature components of the rotor flux in the equations (2-14) we get:

$$\begin{cases} V_{dr} = R_r i_{dr} + \sigma \cdot L_r \cdot \dfrac{di_{dr}}{dt} + e_{dr} \\ V_{qr} = R_r i_{qr} + \sigma \cdot L_r \cdot \dfrac{di_{qr}}{dt} + e_{qr} + e_{\phi} \end{cases} \tag{2-30}$$

With:

$$\begin{cases} e_{dr} = -\sigma L_r g \omega_s \cdot i_{qr} \\ e_{qr} = \sigma L_r g \omega_s \cdot i_{dr} \\ e_{\phi} = s \omega_s \dfrac{MV_s}{\omega_s L_s} \end{cases} \tag{2-31}$$

Replacing the expressions of isd, isq and ψsd in the expression of the electromagnetic torque in equation (2-18) we get:

$$T_{em} = -\frac{pMV_{sq}}{\omega_s L_s} i_{rq} \tag{2-32}$$

2.7.2.3. Expression of active and reactive power of synchronous frame

Taking into consideration the chosen reference frame, the active and reactive powers at the stator can be written as follows:

$$\begin{cases} P_s = -\frac{3}{2} \cdot V_{qs} i_{qs} \\ Q_s = -\frac{3}{2} \cdot V_{qs} i_{ds} \end{cases} \quad (2\text{-}33)$$

Replacing the stator currents by their expressions given in (2-25), the equations below are expressed:

$$\begin{cases} P_s = -\frac{3}{2} \cdot V_s \frac{M}{L_s} i_{qs} \\ Q_s = \frac{3}{2} \cdot V_s \left(\frac{\psi_s}{L_s} - \frac{M}{L_s} i_{dr}\right) \end{cases} \quad (2\text{-}34)$$

These last expressions show that the choice of coordinate system (d-q) makes the electromagnetic torque produced by the DFIG, and therefore the stator power, proportional to the current of the rotor axis (q). The stator reactive power, in turn, is proportional to the current of the rotor axis (d) due to a constant imposed by the grid. Thus, these stator powers can be controlled independently of one another. This shows us that we can set up a control rotor current due to the influence of the couplings. Every current can be controlled independently each with its own controller. The reference values for these regulators will be the rotor axis current (q) and the rotor axis current (d) .The block diagram of the control loops of the axis rotor currents (dq) is shown in figure 2.10, regulators used are PI controllers.

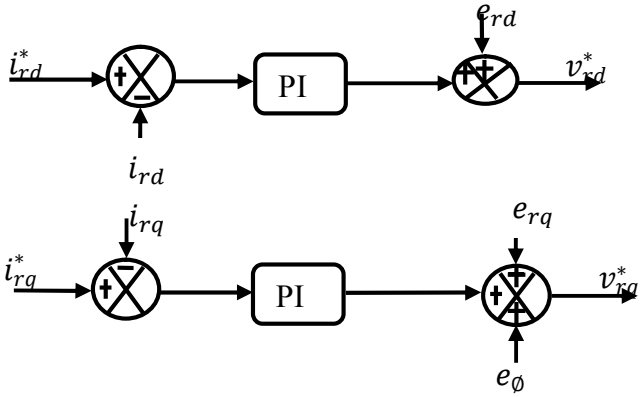

Figure 2.9: Control of rotor currents.

The rotor current of the reference axis (q) is derived from the MPPT control via the stator active power reference. The rotor current of the reference axis (d) is derived from the control of the stator reactive power.

From the equations (2-32) and (2-34) we obtain:

$$\begin{cases} i_{dr}^{*} = -\dfrac{L_s}{M.V_S} Q_S + \dfrac{V_s}{\omega_S.M} \\ i_{qr}^{*} = -\dfrac{.L_s}{M.V_S} P_s \end{cases} \tag{2-35}$$

Figure 2.10 shows the block diagram of the control of RSC.

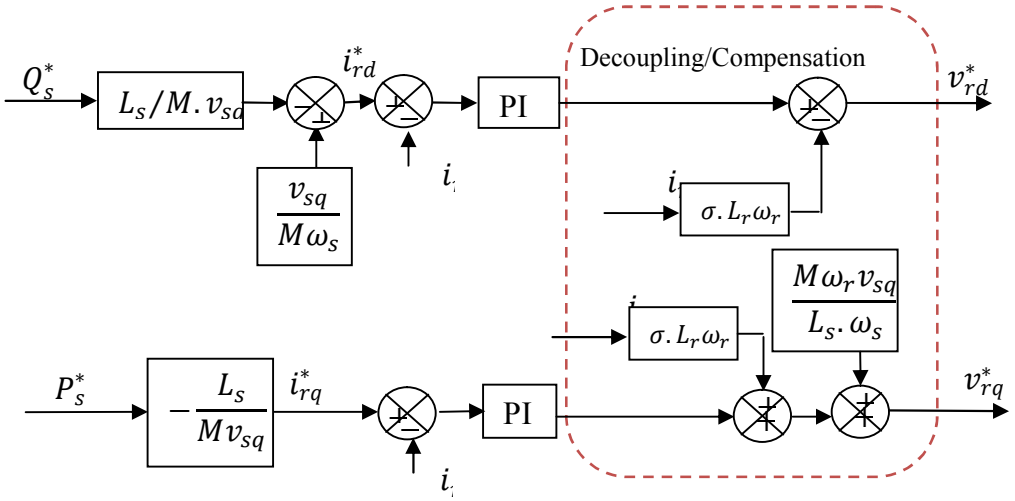

Figure 2.10: Control of rotor side converter.

2.7.3. Control of the grid side converter

The aids of grid-side converter control system are providing bi-directed power flowed channel for control winding grid side converter, the grid side three level converter is to regulate the dc-link voltage and to set a unit power factor [45]. The model of the system is given by the following equation:

$$\frac{d}{dt}\begin{bmatrix} i_a \\ i_b \\ i_c \end{bmatrix} = -\frac{R}{L}\begin{bmatrix} 1 & 0 & 0 \\ 0 & 1 & 0 \\ 0 & 0 & 1 \end{bmatrix}\begin{bmatrix} i_a \\ i_b \\ i_c \end{bmatrix} + \frac{1}{L}\begin{bmatrix} V_a - V_{an} \\ V_b - V_{bn} \\ V_c - V_{cn} \end{bmatrix} \tag{2-36}$$

The dc capacitor voltage equation expressed using switching function is as follows:

$$C\frac{dV_c}{dt} = i_a S_a + i_a S_a + i_a S_a - i_d \tag{2-37}$$

The voltage equations in the d-q synchronous reference frame are presented below:

$$\begin{cases} V_d = Ri_d + L\cdot\dfrac{di_d}{dt} + \omega_s L i_{qr} + V_{dn} \\ V_q = Ri_q + L\cdot\dfrac{di_q}{dt} + \omega_s L i_{dr} + V_{qn} \end{cases} \tag{2-38}$$

The direct axis current is used to regulate the reactive power and the quadratic axis current is used to regulate the DC-link voltage. The reference frame is considered oriented along the

stator voltage vector, this method gives possibility to realise independent control of the active and reactive power between the GSC and the supply side.

For eliminating the current couple between d-axis and q-axis and disturbance of grid voltage, current feedback values ωLiq and ωLid are introduced as compensation components.

2.7.3.1. Phase locked loop (PLL) type estimator

To determine the angles necessary for Park transformation of the stator variables (θ s) and the rotor variables (θ r), we used a phase locked loop (PLL) as showed in figure 2.11. This PLL allows to accurately estimating the frequency and amplitude of the grid [47].

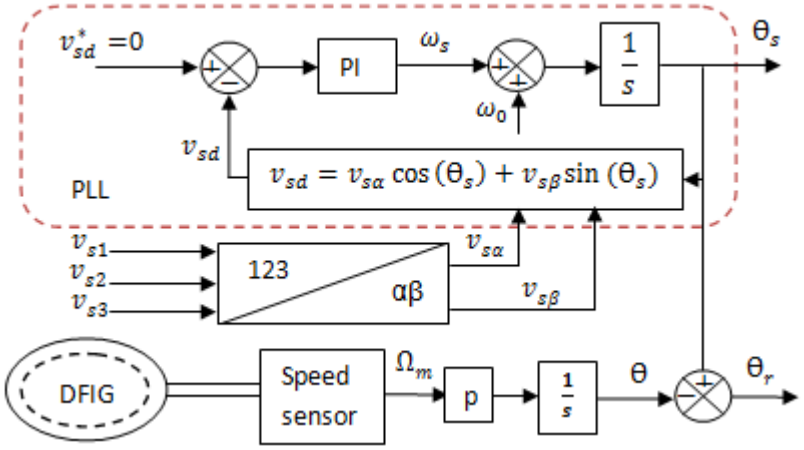

Figure 2.11: Establishment angles processing using a PLL

Based on the above relations, the GSC control diagram can be easily deduced as presented in Figure 2.12.

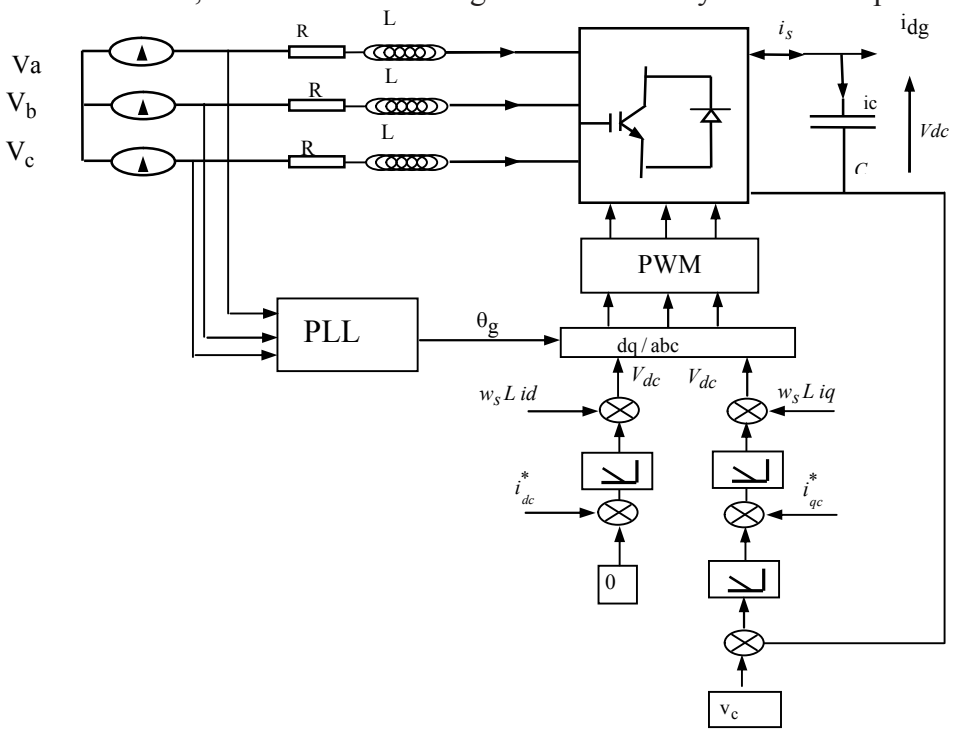

Figure 2.12: Control diagram of the grid side converter.

2.8. Simulation results

To perform the simulation of the DFIG in generating operation, we used the MATLAB-Simulink software, with which we modeled all the parts of the system namely the machine, the inverter, the PWM control, the regulators and various components required for the order. We have subjected the system to reference levels in order to study the behavior of the regulation of the active and reactive powers of the machine transmitted to the network.

The simulation results presented in the figures below with a constant speed of rotation of DFIG equal 50 rad/s.

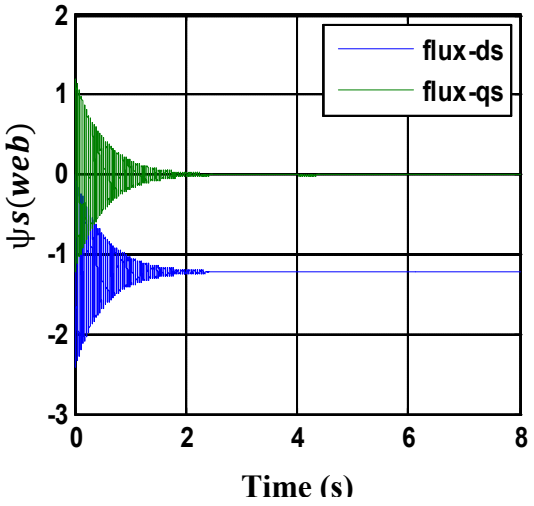

a- Stator Flux

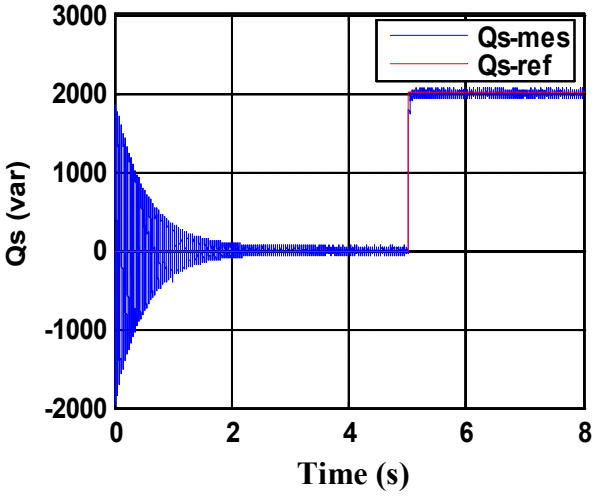

b- Stator reactive power

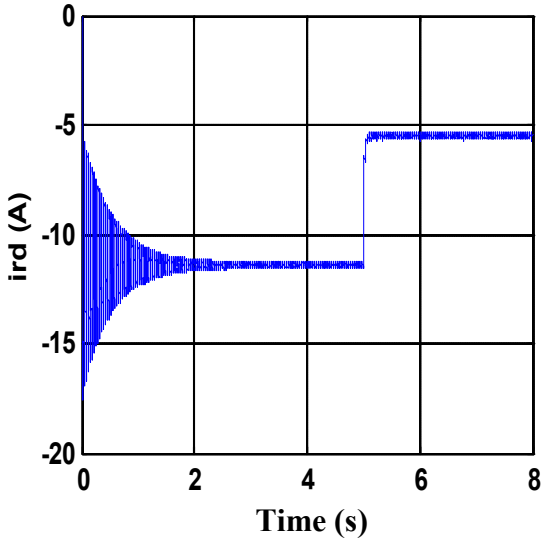

c- Stator current in d-axis

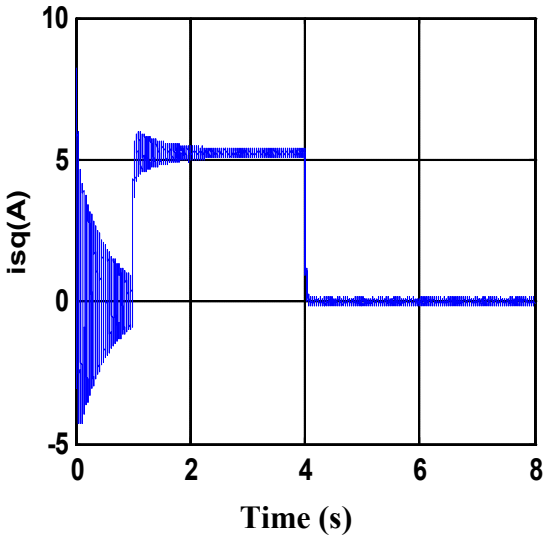

d- Stator current in q-axis

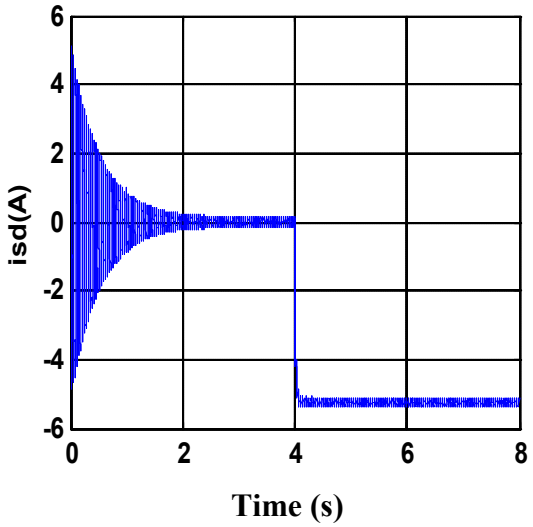

e- *Rotor current in d-axis*

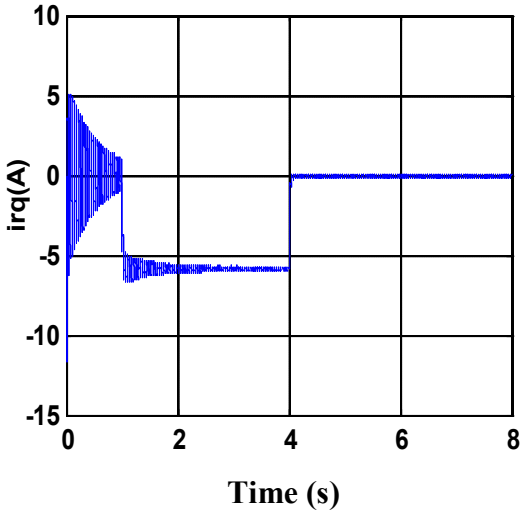

f- *Rotor current in q-axis*

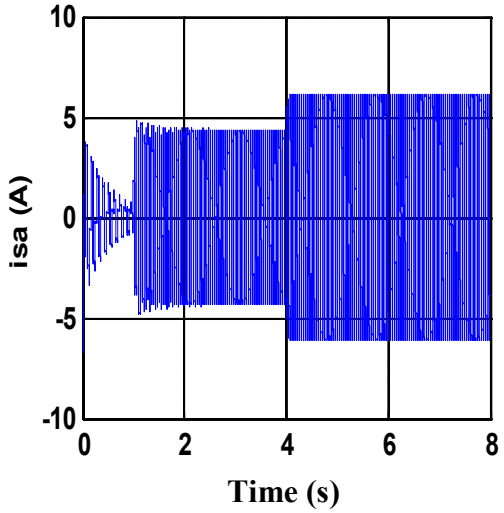

g- *Stator phase current*

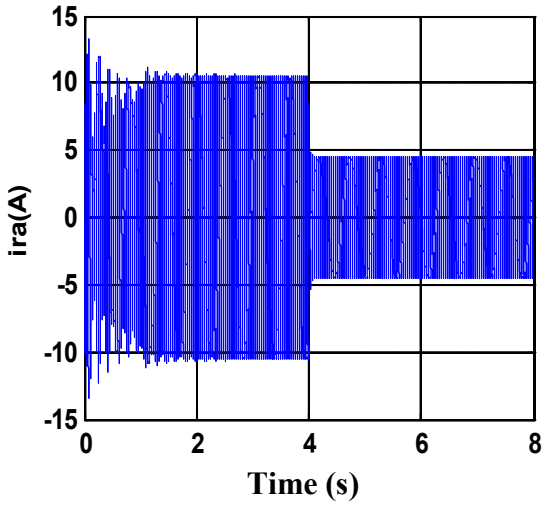

h- *Rotor phase current*

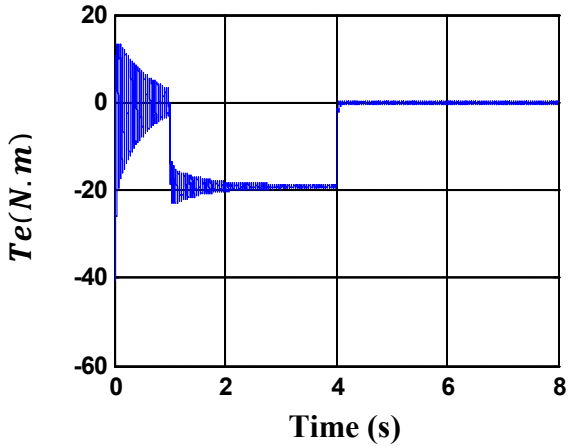

i- *Electromagnetic torque*

Figure 2.13: Simulation results of a vector control of the DFIG.

These simulation results present the different curves obtained by the control of the active and reactive powers generated at the stator of the DFIG, this control makes it possible to decouple the expressions of the active and reactive power of the generator or incurs that of the flux and the torque. We can see that the stator flux follows its reference along the axis (d) with a quadrature component that is almost zero, which means that the decoupling of the machine is done successfully.

2.9. Conclusion

In this chapter, we have studied the electrical and dynamic equations of DFIG used in generator this allowed us to establish a model of Park which reduces the electrical system of the machine from six to four equations.

In the following we have explained the principle of vector control in stator active and reactive power, two regulation loops were presented one regulates the active power and the other regulates the current by PI regulator. A choice on the orientation of the flux was taken by orienting the stator flux along the axis d, therefore the active power will be dependent only Iqr.

At the end of this chapter we have presented the simulation results that are obtained using a two level voltage inverter powered by a voltage continuous considered constant is controlled by pulse width modulation technique (PWM).

CHAPTER THREE

MPPT Control for the Proposed Wind Turbine System

3.1. Introduction

This chapter focuses on the maximum power point tracking (MPPT) control, for the wind energy conversion system. At a given wind velocity, the mechanical power available from a wind turbine is a function of its shaft speed.

To maximise the power captured from the wind, the shaft speed has to be controlled. In order to track maximum power, the matrix converter adjusts the induction generator terminal frequency, and thus, the turbine shaft speed. The matrix converter also adjusts the reactive power transfer at the grid interface towards voltage regulation or power factor correction. Also a MPPT algorithm is integrated in the closed loop control system in order to capture maximum wind power. The claims made for the capabilities of the proposed scheme are supported by analysis and simulation results.

3.2. Modeling of wind turbine

A wind turbine captures the kinetic energy of the wind and converts it into a torque that turns the rotor blades. Three factors determine the relationship between wind energy and mechanical energy recovered by the rotor: air density, rotor swept area and wind speed rotor swept area.

3.2.1. The wind velocity

The daily variation of the wind speed is due to thermal phenomena related to solar radiation. The average wind speed varies little at night and increases during the day from sunrise. Seasonal or monthly variations in wind speed depend on geographical location and differ from one site to another. Only meteorological records of wind parameters over a long period can characterise these variations.

3.2.2. Power recoverable by a turbine

The turbine which has three blades of length R, fixed on a drive shaft rotating at a speed Ω, which will drive a generator (DFIG) through a gain speed multiplier G. Figure 3.1 shows the diagram of a wind turbine. Wind energy comes from the kinetic energy of the wind. Indeed, if we consider a mass of air m, which moves with velocity v, the kinetic energy of this mass is:

$$E_c = \frac{1}{2}mv^2 \qquad (3-1)$$

If, during the unit of time, this energy could be completely recovered by means of a propeller which sweeps a surface S, situated perpendicularly to the direction of the wind speed, the inst-antaneous power supplied would be:

$$P_{wind} = \frac{1}{2}\rho \cdot S \cdot V_{wind}^3 = \frac{1}{2}\rho \cdot \pi \cdot R^2 \cdot V_{wind}^3 \qquad (3-2)$$

With:

ρ: Density of air (this is 1.25 Kg / m in a normal atmosphere).

S: It is the circular surface swept by the turbine, the radius of the circle is determined by the length of the blade.

R: practically corresponds to the length of the blade.

V_{wind}: is the wind speed in (m/s).

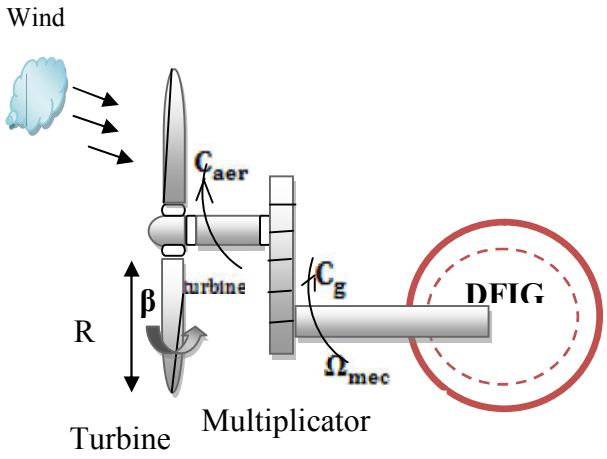

Figure 3.1: Scheme of a wind turbine.

From the relation (3-2) noted that the power is directly proportional to the surface swept by the rotor, but especially to the cube of the wind speed.

However, all the energy cannot be captured; we cannot extract all the power because the wind speed is not zero after the wind turbine. A coefficient Cp is then introduced, which depends on the aerodynamic characteristics of the blades. This coefficient corresponds to the rotor efficiency of the wind turbine [48,49,50]. The power on the rotor shaft or the aerodynamic power appearing at the rotor of the turbine is written:

$$P_{air} = C_P P_v = \frac{1}{2} C_P(\lambda, \beta)(\rho S v^3) \qquad (3-4)$$

Cp : Power coefficient defined as follows:

$$C_p = 7{,}9563 \cdot 10^{-5}\lambda^5 - 17{,}375 \cdot 10^{-4}\lambda^4 + 9{,}86 \cdot 10^{-3}\lambda^3 + 9{,}4 \cdot 10^{-3}\lambda^2 + 6{,}38 \cdot 10^{-2}\lambda + 0.001 \qquad (3-5)$$

β : orientation angle of the blades.

λ: is the speed ratio defined as:

$$\lambda = \frac{\Omega_t R}{V_{wind}} \qquad (3-6)$$

R: Blades length.

Ω_t:Speed of the turbine.

V_{wind}: Wind speed (m/s)

The aerodynamic torque is given by:

$$T_{air} = \frac{P_{air}}{\Omega_{turine}} = C_P \frac{\rho\, Sv^3}{2} \cdot \frac{1}{\Omega_{turbine}} \qquad (3-8)$$

3.2.3. The power coefficient

The Cp represents the ratio of the recovered power to the recoverable power. This coefficient has a maximum of 16/27 or 0.59 [41, 45]. It is theoretical limit called Betz limit that sets the maximum extractable power for a given wind speed. This limit is in fact never reached and each wind turbine is defined by its own power coefficient expressed as a function of the relative speed λ.

The characteristics of Cp as a function of different values of the wedging angle are illustrated in figure 3.2.

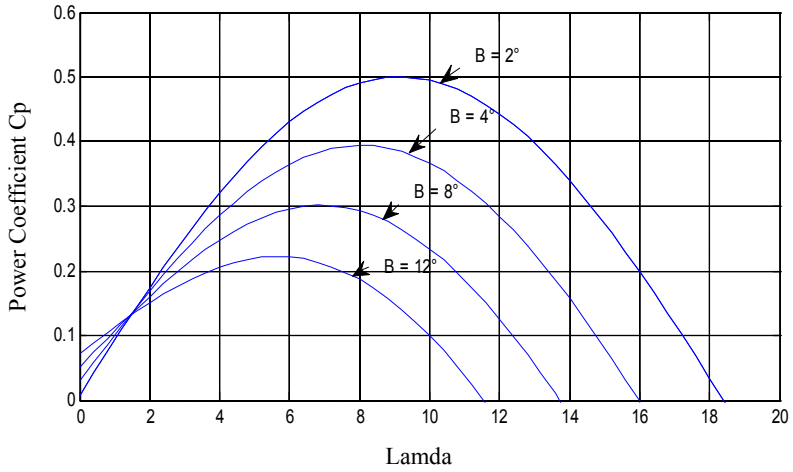

Figure 3.2: Development of power factor of the wind turbine (fixed angle of setting).

3.2.4. Model of multiplier

The multipliers currently used two to three epicyclic gear trains to obtain multiplication ratios of the order of 100. These gears are noise generators and mechanical losses [42].

The purpose of the multiplier is to adapt the slow speed of the turbine to the speed of the generator, and to be able to model it, we will use a speed gain G which corresponds to the multiplication ratio.

$$T_g = \frac{T_{aero}}{G} \quad (3-9)$$

With:

T_g: Torque from the multiplier.

T_{aero}: Aerodynamic torque.

G : Gain of multiplier

For speed, we will have:

$$\Omega_{turbine} = \frac{\Omega_{mec}}{G} \quad (3-10)$$

3.2.5. Dynamic equation of shaft

The modeling of the mechanical transmission is summarised as follows [43]:

$$J_t \frac{d\Omega_{mec}}{dt} + f_{mec} = \sum Torques = T_{mec} \quad (3-11)$$

Where:

J_t: The moment of inertia of the turbine equivalent to the inertia of the three blades of the wind turbine.

f : Coefficient of viscous friction.

T_{mec}: The mechanical torque, the latter takes into account:

The electromagnetic torque produced by the generator Tem;

The viscous friction torque T_{vis}, and the torque from the multiplier T_g

3.3. Scheme of turbine model

The turbine generates an aerodynamic torque transmitted to the multiplier. This torque can be calculated from the values of the wind speed and the rotational speed of the turbine.

The multiplier transforms turbine speed and aerodynamic torque respectively into mechanical speed and torque of the multiplier.

The turbine can be controlled by the action of the electromagnetic torque of the electric converter. Wind speed is considered a disturbance figure 3.3.

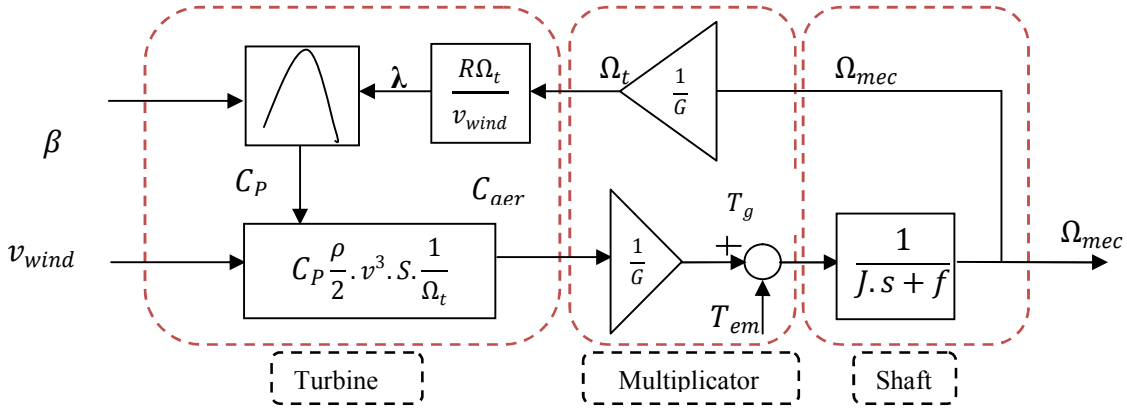

Figure 3.3: Block diagram of the turbine model.

3.4. Control strategy of turbine

As illustrated in figure 3.4, there are four (04) main areas of operation.

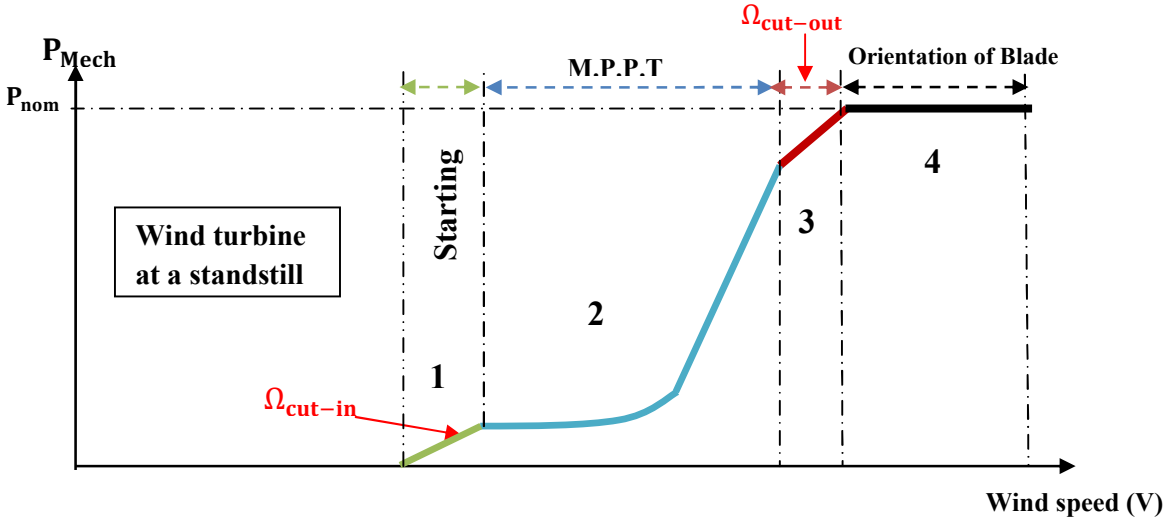

Figure 3.4: Wind turbine control strategy based on four speed regions.

- **Zone1**: This is the starting area of the machine, it starts when the mechanical speed reaches a minimum value. (This is the mechanical speed of the generator for which wind turbine has started).

- **Zone2**: When the speed of the generator reaches a threshold value, a control algorithm for extracting the maximum power MPPT (Maximum Power Point Tracking). To extract the maximum power, the angle of the blade is kept constant at its minimum value in order to obtain a maximum Cp. In this zone, the mechanical speed varies and can reach a value close to the nominal speed, the electrical power increases rapidly.

- **Zone3**: In this zone the wind turbine runs at constant speed, and the power of the generator reaches higher values up to 90% of the nominal power Pnom.

- **Zone4**: At the nominal power Pnom, a limitation of the generated power is carried out using a system of orientation of the blades. (calibration angle) is the 'Pitch Control'
- We are interested in the zone 2 or the maximisation of the electrical energy extracted; this operation is carried out by the control of the electromagnetic torque to generate.

3.5. Algorithms for maximising extracted power

The purpose of the variable speed control of the DFIG is to extract the maximum wind power. For this, we need algorithm acting on the set point variables in order to have the best possible performance of the studied device.

Through the bibliography we have distinguished two families of control structures for the maximisation of extracted power:

- With control of the mechanical speed.
- Without control of the mechanical speed.

It is difficult to accurately measure the wind speed which is of a very fluctuating magnitude. An erroneous measurement of the speed leads to a degradation of the power captured according to the MPPT technique. This is why most wind turbines are controlled without speed control [47].

- **Maximisation of power without speed control:**

This control structure is based on the assumption that the wind speed varies very little in steady state. In this case we obtain:

$$J_t \frac{d\Omega_{mec}}{dt} = T_{mec} = 0 = T_g - T_{em} - T_{vis} \qquad (3-12)$$

If we neglect the effect of torque viscous friction$T_{vis} \cong 0$, we obtain:

$$T_{mec} = T_g \qquad (3-13)$$

From the measurement of the mechanical speed and the knowledge of an estimation of the speed of the wind, we obtain:

$$\mathrm{C_{air}} = \mathrm{C_P} \frac{\rho\, \mathrm{S}}{2} \frac{1}{\Omega_{\mathrm{turbine-est}}} \mathrm{V_{est}^3} \qquad (3-14)$$

With: $$V_{est} = \frac{\Omega_{turbine-est} \cdot R}{\lambda} \qquad (3-15)$$

The speed ratio set to the value λ_{Cpmax}, which corresponds to the maximum of the power coefficient C_{pmax} and, by grouping the previous equations; we will have the expression of the reference torque which is proportional to the square of the speed of the generator.

$$T_{em-ref} = \frac{C_P}{\lambda^3_{Cp\,max}} \cdot \frac{\rho \pi R^3}{2G^3} \Omega^2_{mec} \qquad (3-16)$$

Figure 3.5 shows the maximisation block diagram of the extracted power without speed control.

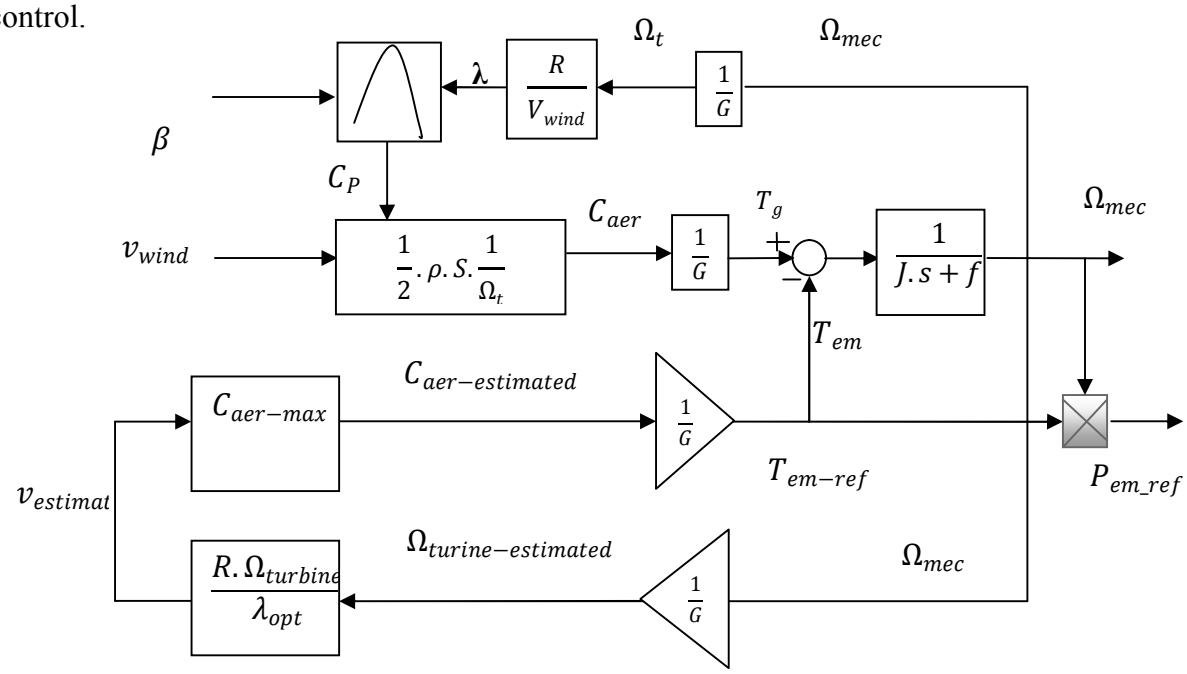

Figure3.5: Block diagram of the maximisation of extracted power without speed control

3.6. Simulation Results

The simulations without speed control were carried out with the software Matlab / simulink, in order to validate the control studied in this chapter. Different wind speed is applied to the blades of the wind turbine. The reference voltage of the DC bus, denoted Vdc.. The reference reactive power Qs is set to 0. We show that the different powers involved can be controlled independently.

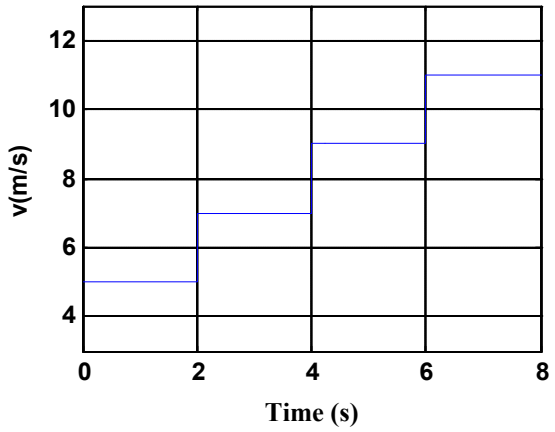

a- Wind speed as a function of time

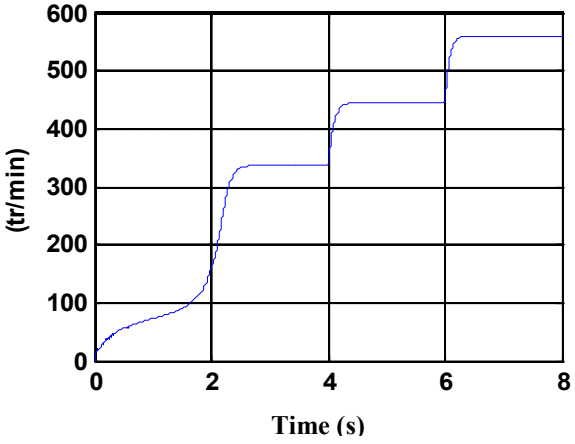

b- *Variation of the mechanical speed (tr/min)*

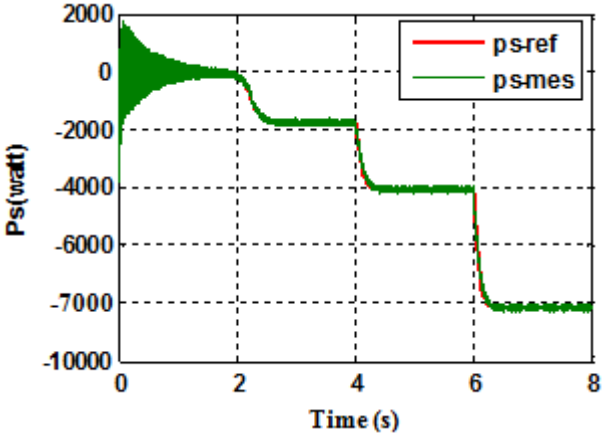

c- Stator active power

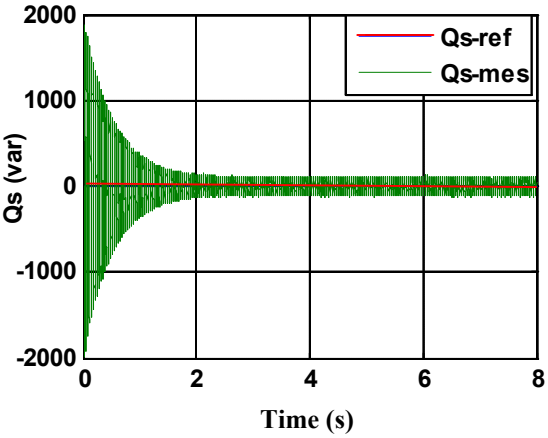

d- Stator reactive power

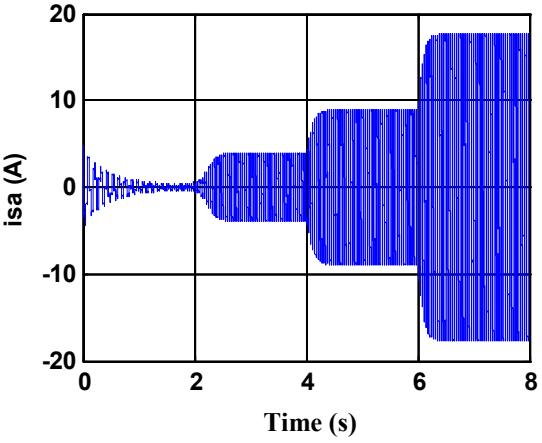

d- *Current of a stator phase*

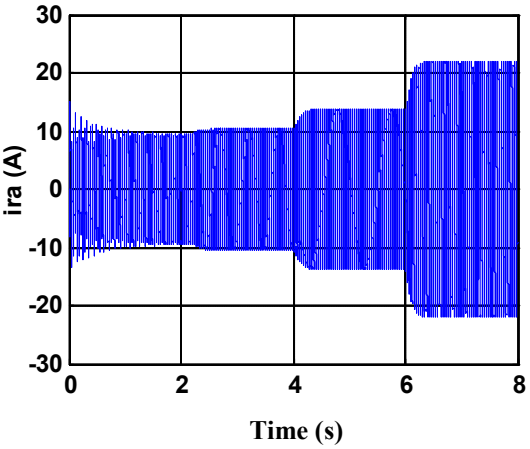

e- Current of a rotor phase

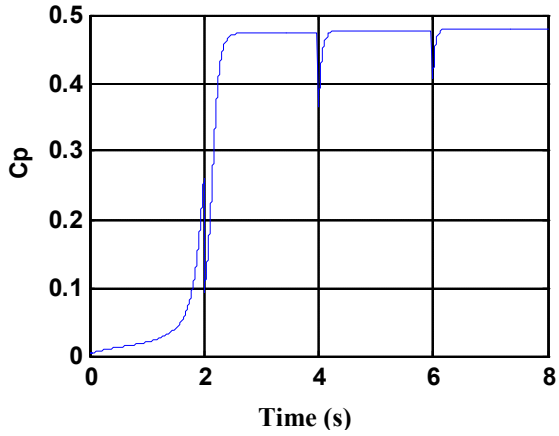

f- Power Coefficient of the turbine

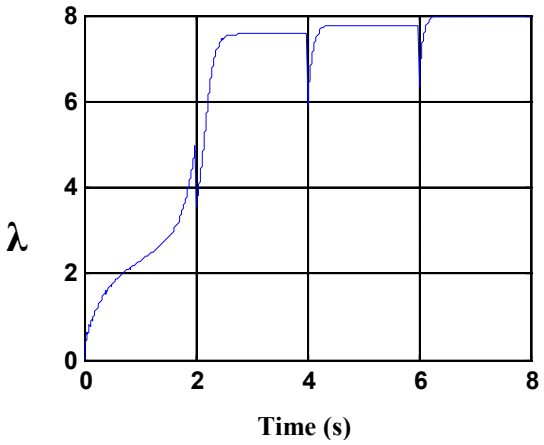

g- Relative velocity of the wind turbine

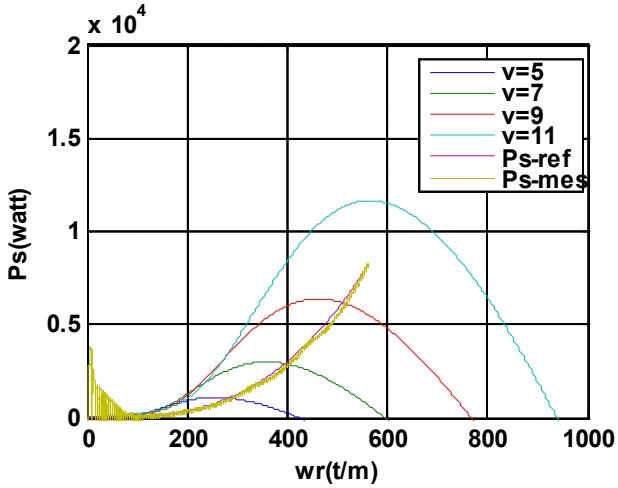

h- Characteristic of the wind turbine in the power plan, rotation speed

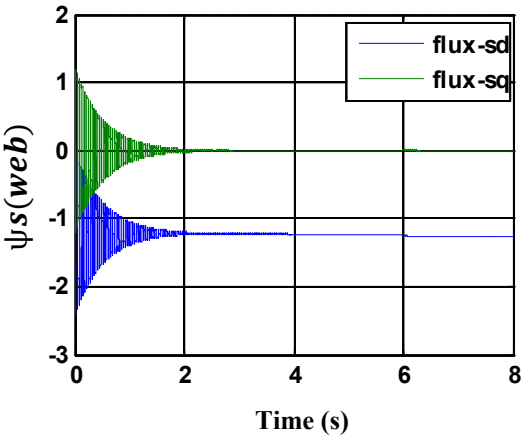

i- Stator Flux of DFIG

Figure 3.6: Simulation result of a wind energy conversion chain (without mechanical speed control)

The profile of the applied wind is given in figure 3.6-a above. From the results obtained for this application, we distinguish the following remarks:

The specific velocity λ and the power coefficient Cp figure 3.6 do not change many values, they remain practically equal to their optimum reference values 8.1 and 0.48 successively.

The shape of the components of the stator flux shows a good flow orientation guaranteeing a well decoupled vector control of the DFIG.

The stator reactive power is zero it is a condition of operation of the DFIG to have a unit power factor.

The stator current supplied by the DFIG is in phase opposition with respect to the mains voltage, since the DFIG only injects the active power into the network ($Q_{p\_ref} = 0$).

We find that during the operating mode the current of the filter is in phase with the mains voltage, this means that the DFIG absorbs an active power of the network.

Note that the DC bus voltage stabilises on its reference value imposed by the command.

The DC voltage output of the rectifier is well controlled and almost insensitive to variations in speed.

3.7. Conclusion

This chapter presented a maximum power point tracking method of the proposed wind turbine system. The controller including the MPPT method controls the shaft speed to maximise the power captured from the wind. The system of orientation of the blades applied to limit the power generated at the stator of the DFIG.

Thus, the DFIG indicats that is able to ensure, by its variable speed operation, a maximum power output. This has been observed through the increase of the power coefficient as a function of time and the characteristic of power speed rotation.

CHAPTER FOUR

Sensorless Control of DFIG using MRAS

4.1. Introduction

The control of the DFIG is based on the measurement of its stator and rotor currents, the speed or the position of the rotor, physical quantities which must provide sufficient information in quality and quantity of the machine model.

The position of the rotor as well as its speed is generally obtained with the help of an incremental encoder. In addition to its cost, this sensor poses, among others, the following problems:

- To avoid significant quantisation errors, the encoder must be sufficiently accurate.
- To operate in harsh environments, the encoder must be protected from dust and mechanical shock.
- The encoder must be placed between the load and the machine shaft. This will induce an increase in the distance between these two elements, so a longer elastic coupling. In addition, it must support the jolts of torque imposed by the machine.

For all these reasons, it is interesting to study the removal of the mechanical sensor and to replace it with estimators or observers of the speed or the position based on the measurement of the electrical quantities of the machine.

In this chapter, we study an estimator using the model reference adaptive system (MRAS) method.

4.2. The different methods of estimating the mechanical speed

4.2.1. Estimation of the speed with the machine model

- **The estimation methods**

The estimation methods known rely on state model duplication in the control part to reconstruct internal variables that are inaccessible on the real system. Many of the methods proposed in the literature deal with the control of sensorless speed of the machine [39].

- **Method based on the autopilot law**

The speed estimation method uses the autopilot law of electrical machines and can be easily implemented. It is based in the case of the fundamental relationship between the natural frequencies of the induction machine. The objective of this method is to obtain the electric speed of the rotor from the two other frequencies of the motor, which can be estimated. These estimations are evaluated from the measured stator currents and the estimated rotor fluxes (magnetising currents) of the motor [53].

- **Model reference adaptive system (MRAS)**

The model reference adaptive system is based on comparing the output of two estimators. The first, which does not introduce the magnitude to be estimated (the speed in our case), is called reference model and the second is the adjustable model. The error between these two models drives an adaptation mechanism that generates the speed. The latter is used in the adjustable model [40, 53].

- **Observer method**

The problem of open loop processing can be avoided by using observers to reconstruct the model of the system. In fact, an observer is only a closed loop estimator that introduces a gain matrix to correct the error on the estimation. In order to be able to observe the non measurable quantities of the machine, it is necessary that the system be observable. Different structures of observer models have been proposed in literature. They are very attractive and give good performance in a wide range of speed [52].

- **Deterministic observers**

In practice, the deterministic observer takes two different forms, a reduced order observer where only non measurable variables of the model system are reconstructed, and the full order observer for which all system variables are rebuilt. Observers have an additional input which possibly ensures the exponential stability of the reconstruction, and imposes dynamic convergence. The performance of this structure obviously depends on the choice of the gain matrix [52].

- **Extended Kalman Filter (EKF)**

One of the methods used to estimate the speed of the induction machine is the Extended Kalman Filter (EKF). The Kalman filter is a closed loop non linear observer whose gain matrix is variable. At each computation step, the Kalman filter predicts the new values of the state variables of the asynchronous machine (stator current, rotor flux and speed). This prediction is performed either by minimising the noise effects and modeling errors of the parameters or state variables or by a genetic algorithm [56].

4.2.2. Estimation of the speed without machine model

- **Estimation of the speed from the salient of the machine**

Generally, induction machines are theoretically designed symmetric and should not have salient. So the machine has salient due to construction inaccuracies (such as eccentricity), the existence of rotor slots and the saturation phenomenon. The salient present in a machine

introduce a spatial variation of the parameters (resistance or inductance), and allow the current or the voltage to contain information on the position of these projections and consequently the position of the rotor, therefore information on the speed [52, 53]. Various techniques can be enumerated for the estimation of the speed using this physical data of the machine related to the presence of salient. The insensitivity with respect to the parameters of the machine is one of the great advantages for these techniques in return for the requirement of high performance means in terms of signal processing. The challenge remains in real time estimation, especially for looped orders.

- **Estimation based on artificial intelligence**

Genetic algorithms, fuzzy logic and neural networks are all artificial intelligence based numerical computation techniques, which are popular in the field of computing. But, increasingly, applications based on these new numerical computation approaches are developing for practical applications in the fields of science and engineering [46]. Observers or estimators based on artificial intelligence techniques provide better dynamics, better accuracy and are more robust [47, 48, 49]. Their robustness is very good even for important variations of the parameters of the machine. Nevertheless, the need for perfect knowledge of the system to be adjusted or estimated and the lack of system expertise limit current applications to a very specific range.

4.3. Sensorless control of DFIG system using MRAS observer

4.3.1. The MRAS method

The principle of estimation by this method is based on the comparison of the quantities obtained in two different ways, on the one hand by a calculation that does not depend explicitly on the speed (reference model) and on the other hand by a calculation that is explicitly dependent on speed (adaptive model). This method developed by Schauder [39, 40, 53] is known as Model Reference Adaptive System (MRAS).

For the estimation of the speed, it proposes the comparison of the estimate of the common flow obtained with the stator equations (independent explicitly of the speed) and on the other hand with the rotor equations (dependent explicitly on the speed).

The objective is to find the speed parameter of the adaptive model to ensure the results of the two identical rotor flux estimates. Thus the value of the estimated speed becomes that of the real speed. The proper functioning of the estimation is ensured by a judicious choice of the adaptation function to converge the adaptive model towards the reference model based on the

Popov criterion [53]. The scheme of this method is summarised in figure 4.1. This method has a drawbacks, it uses only observed flux quantities to reconstruct the value of the speed. This is why we prefer to apply another approach proposed by Yang [40, 44] which considers the measurements of the currents and the fluxes estimated as output quantities of the reference model (real asynchronous machine). This choice allows better accuracy since the model must converge to the output quantities of the actual machine.

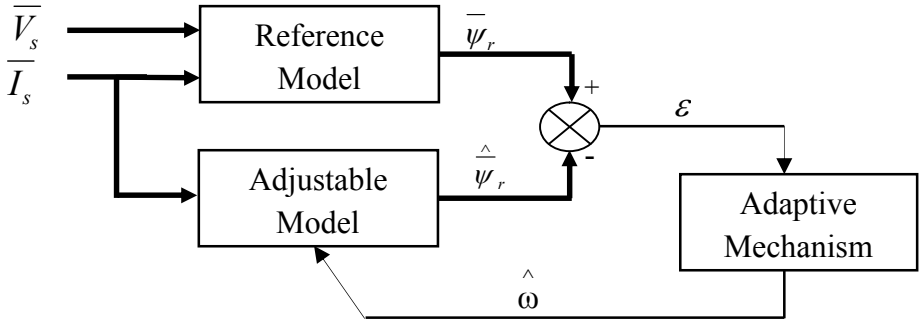

Figure 4.1: MRAS scheme for speed estimation.

4.3.2. MRAS estimation of mechanical quantities of DFIG

A MRAS estimator is used to estimate the rotational speed and rotor position of the DFIG and the structure for this estimator is depicted in figure 4.2. The MRAS estimator is the stator - flux error vector which is fed to the adaptation mechanism to ensure that the system will be stable and the estimated quantity will converge to the ideal (actual) value [39, 40, 44, 53].
The equations of the chosen reference model and adaptive model are given by:

- **Reference model**

$$\frac{d\,\overline{\psi}_{dr}}{dt} = \frac{L_r}{M}\left(\overline{V}_{ds} - R_s\,\overline{i}_{ds} - \sigma\,L_s\,\frac{d\,i_{ds}}{dt}\right) \tag{4-1}$$

$$\frac{d\,\overline{\psi}_{qr}}{dt} = \frac{L_r}{M}\left(\overline{V}_{qs} - R_s\,\overline{i}_{qs} - \sigma\,L_s\,\frac{d\,i_{qs}}{dt}\right) \tag{4-2}$$

- **Adaptive model**

$$\frac{d\,\hat{\overline{\psi}}_{dr}}{dt} = V_{dr} - \frac{1}{T_r}\hat{\overline{\psi}}_{dr} - \hat{\omega}\,\hat{\overline{\psi}}_{qr} + \frac{M}{T_r}\overline{i_{ds}} \tag{4-3}$$

$$\frac{d\,\hat{\overline{\psi}}_{qr}}{dt} = \overline{V_{qr}} - \frac{1}{T_r}\hat{\overline{\psi}}_{qr} + \hat{\omega}\,\hat{\overline{\psi}}_{dr} + \frac{M}{T_r}\overline{i_{qs}} \tag{4-4}$$

The error between the two models is given by:

$$\overline{\varepsilon} = \overline{\psi_r} - \overline{\hat{\psi}_r} \tag{4-5}$$

For the improvement of the estimation response a PI controller has been proposed for error minimisation

$$\hat{\omega} = K_p\left(\psi_{rd}\hat{\psi}_{rq} - \psi_{rq}\hat{\psi}_{rd}\right) + K_i\int\left(\psi_{rd}\hat{\psi}_{rq} - \psi_{rq}\hat{\psi}_{rd}\right)dt \tag{4-6}$$

With: K_p , K_i , positive constants.

The structure of the speedless control of the doubly fed asynchronous machine by the speed estimation method according to the MRAS principle is shown in figure 4.2.

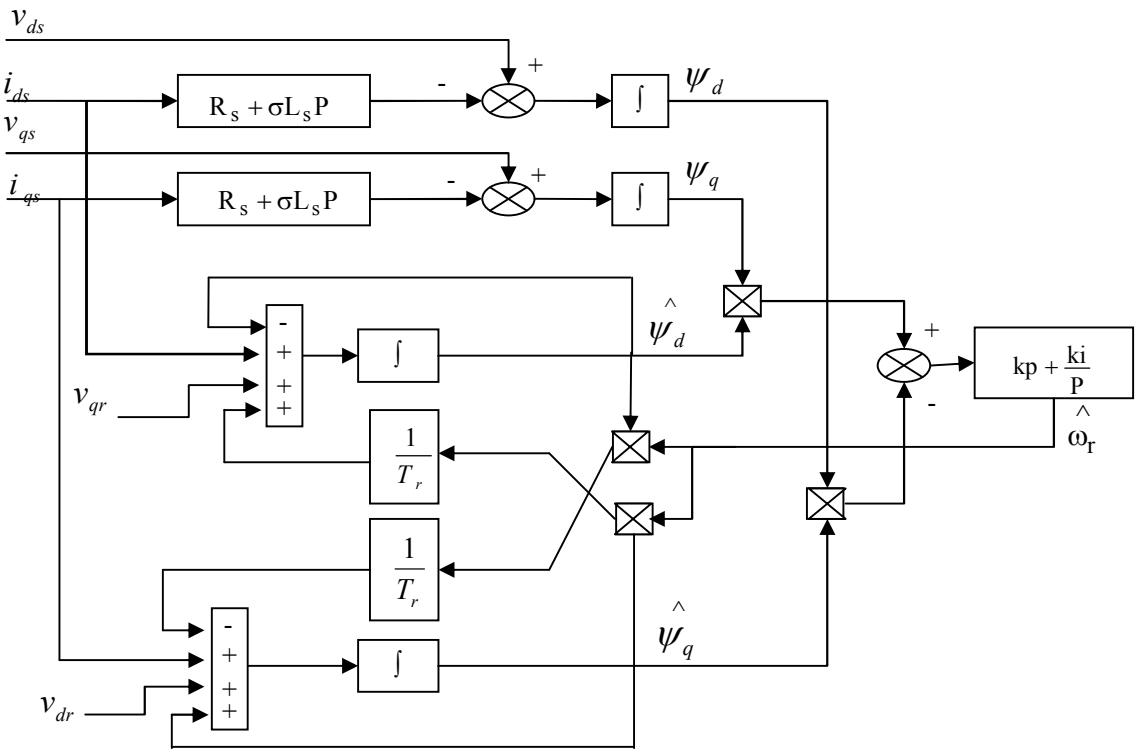

Figure 4.2: Scheme of Principle of the MRAS Observer.

4.4. Global scheme of the vector control of DFIG without sensors

The overall scheme of the DFIG control without mechanical sensors is shown in figure 4.3.

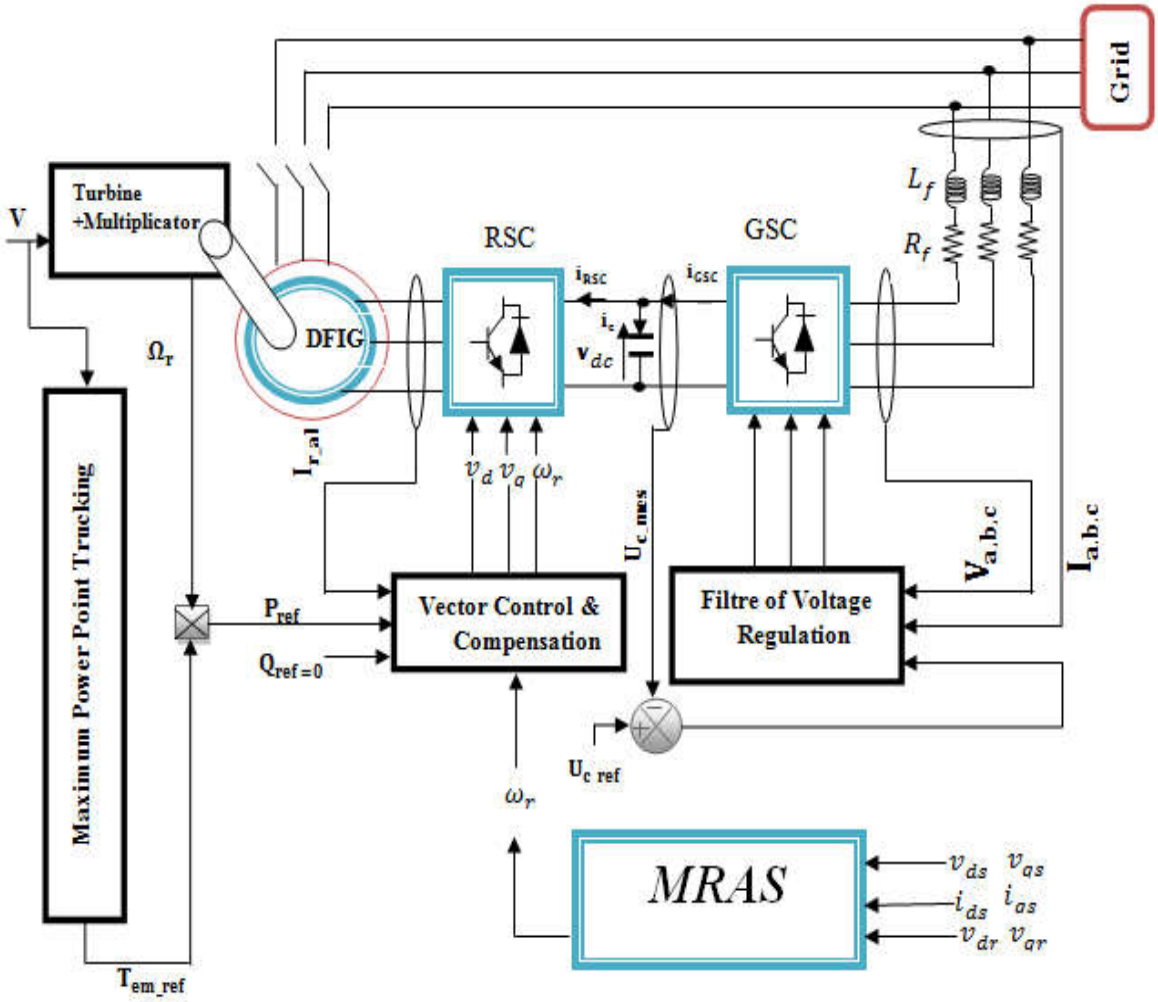

Figure 4.3: Block diagram of sensorless vector control of the DFIG using (MRAS).

4.5. Simulation Results

The wind parameters are: β=0, $R_t = 3m$, the optimal tip speed ratio $\lambda_{opt} = 8.1$, Otherwise the speed increase ratio of the gearbox G=2, the parameters of the DFIG used for simulation are given in appendix A. The simulations were implemented with Matlab/simulink platforme for a step of sampling time T=2x10^{-5}.

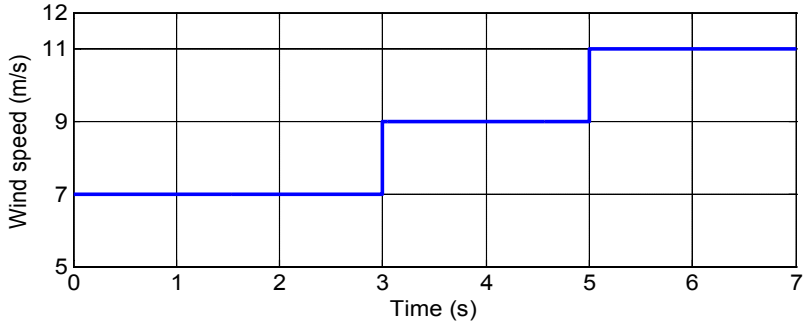

a- *Wind speed as a function of time*

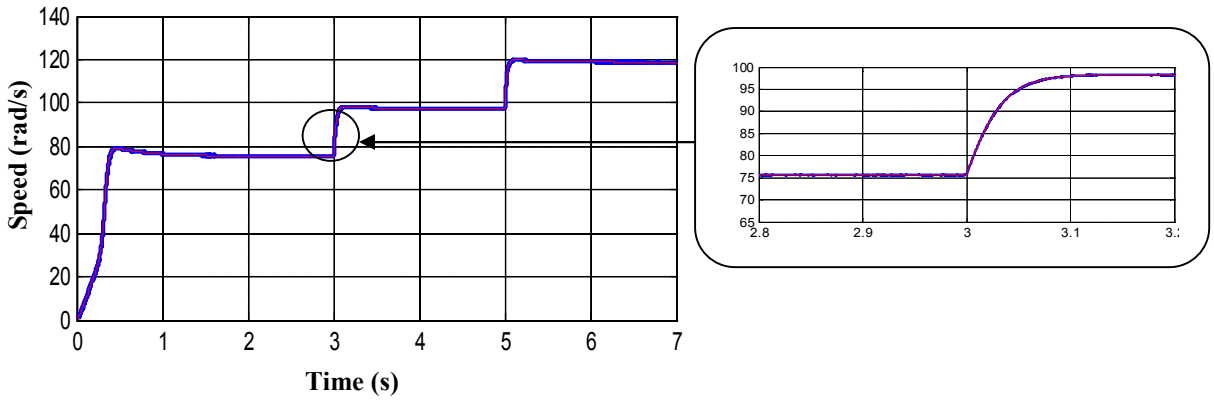

a- The estimated rotor speed by MRAS with Zoom

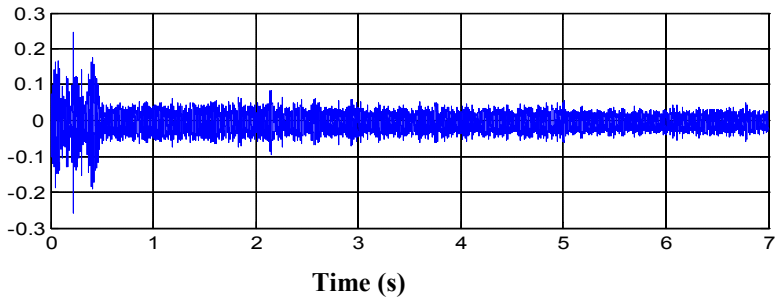

b- The estimated speed error

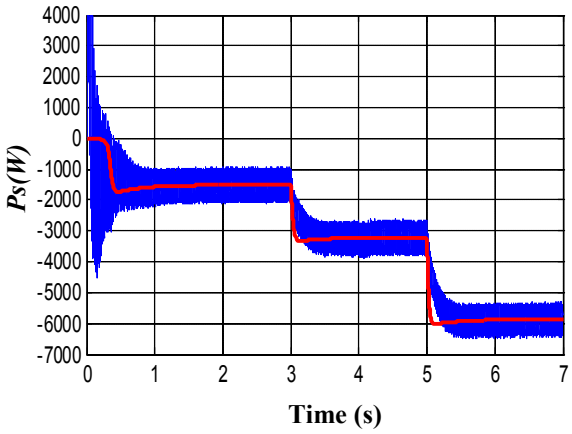

c- Stator active power and its reference

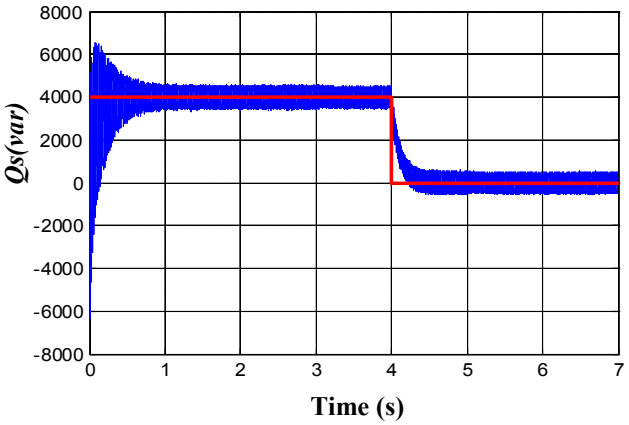

d- Stator reactive power and its reference

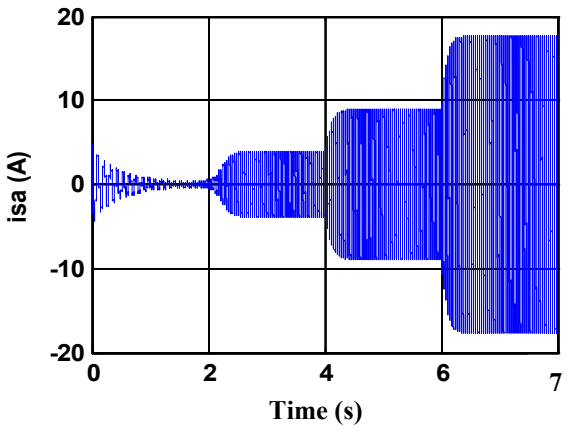

e- Stator phase current

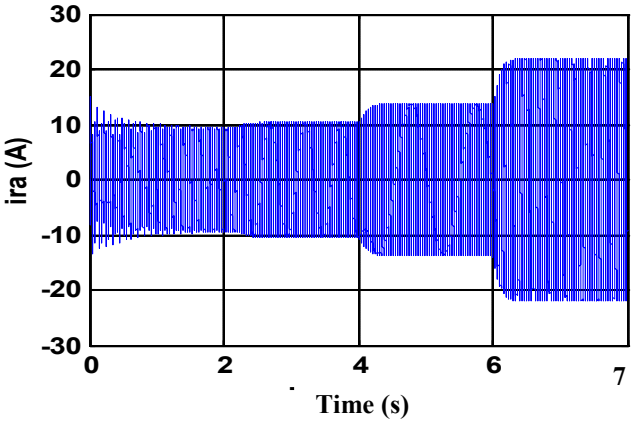

f- Rotor phase current

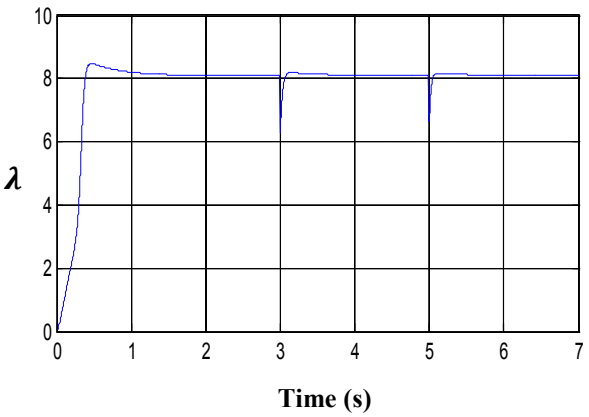

h- Relative velocity of wind turbine

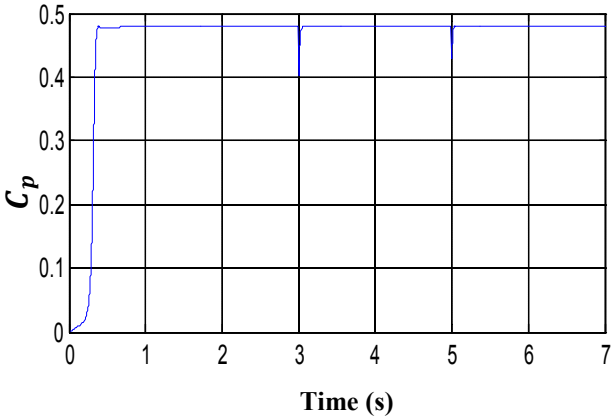

g- Power Coefficient of turbine

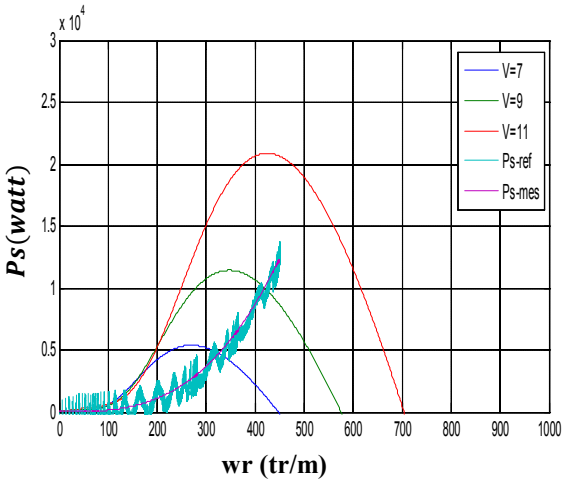

i- Wind turbine Characteristics Of power with rotation speed

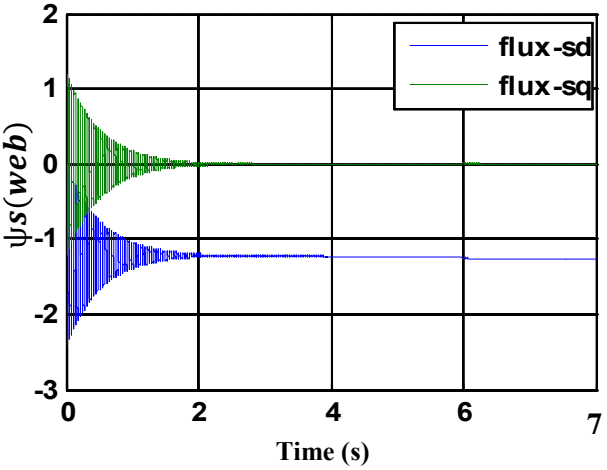

g- Stator Flux of DFIG

Figure 4.4: Simulation results for positioning the rotor without sensor by using MRAS observer.

The simulation results make it possible to observe the evolution of different quantities involved, where the figure 4.4(a) shows the dynamic process of estimated rotor speed tracing wind speed, the performance of MRAS observer tracking the rotational speed, also the rotor speed error indicate excellent tracking performance in figure 4.4(b). The stator active and reactive power are shown in figure 4.4(c,d) which represent a good track with its references and verify the decoupling between the active and reactive power, except in the first shows of the oscillations during the transient response and the active power output of the generator increases proportionally according to increasing of the wind speed values. Figure 4.4 (h,g) shows that when the wind velocity varies suddenly Cp can fast reach around the optimal value, the power coefficients Cp remain practically equal to their optimal reference values which is Cpmax=0.48 which is occurs at λopt=8.1.

The amplitude of both rotor and stator current in figure 4.4 (e, f) changed during the period of active and reactive power variation, even the frequency of stator current is constant according to power frequency of the grid with amplitude change when the reference of the active power is modified.

Figure 4.4 (i) illustrates the rotor speed power characteristics of DFIG according with the optimal value, these results realise the maximum wind energy tracking control. Therefore to extract the maximum power references with the control mechanism of the maximal wind energy capturing, so that optimal tip speed ratio is maintained for maximum power capture and the generator active power matches up to the output power of the turbine.

Consequently, can be observed that the simulation result of the estimated values with MRAS observer for rotor speed is useful and in good agreement with those obtained from actual.

4.6. Conclusion

This chapter has presented a sensorless control strategy for doubly fed induction generator in variable speed wind turbines application based MRAS observer, which implemented in a vector control without a speed sensor.

The results of the simulation obtained for the estimation of the speed are satisfied as point of view in estimation error, robustness and stability of the global drive system.

Concerning speed based operation; these results showed that the characteristic of the speed estimated by the MRAS shows a good dynamic response.

General Conclusion

The objective of our work was to make a modeling and control of a doubly fed induction generator based wind turbine generator system, and then uses these models to develop a control system with its sensor that was to achieve and ensure optimal efficiency of operation. More specifically, the modeling of different components, the control strategies for the RSC and GSC converters have been studied and analysed for improves and contributes to the quality of the network.

As a basis of the research, the model of a wind turbine generator system equipped with a doubly fed induction generator based on MRAS observer was developed in a Matlab/ Simulink environment, which make it possible to have a decoupling and an independent control of the active and reactive power. The field oriented control was realised in the rotor side converter. On one hand, it has allowed us to improve the dynamic and static performance of the DFIG and, on the other hand, to ensure robustness control.

Finally, this contribution study with simulation encourages for further research of state estimation used MRAS observer for sensorless MPPT control and fault detection in wind energy conversion systems, interesting prospects that could contribute to the improvement of function of the DFIG which provided using another algorithms of the power captured by various techniques: Fuzzy logic, Genetic algorithm, Neural network.

Appendix A

1.Doubly fed induction machine parameters:

Rated power, Pn	7.5KW
Stator resistance, Rs	0.474 (Ω)
Rotor resistance, Rr	0.7614 (Ω)
Mutual inductance, M	0.107 (H)
Stator inductance, Ls	0.12 (H)
Rotor inductance, Lr	0.122 (H)
Number of pair of poles, P	2
Utilised grid voltage	220V
Frequency of grid	50 Hz

Table A.1: Doubly fed induction machine parameters.

Turbine parameters:

Number of blades	3
Blade diameter	3 m
Gain of multiplicator	2
Moment of inertia	0,5 Kg.m²
Viscous friction Coefficient	0.0024*N.m.s/rad*

Table A.2: Turbine parameters.

PWM converter parameters:

Input ac rated phase-voltage: Vinp=220V/f=50Hz, DC link capacitance: C=0.002f, AC filter inductance: L=0.014H; Resistance: r = 0.3 Ω .

Appendix B

Calculation of PI controller parameters

In our work, we are interested in the design method which is based on the compensation of the time constant of the regulator with that of the process of the quantity to be regulated. Figure (B.1) shows a system for adjusting each power at the stator level of the closed loop DFIG by a PI controller.

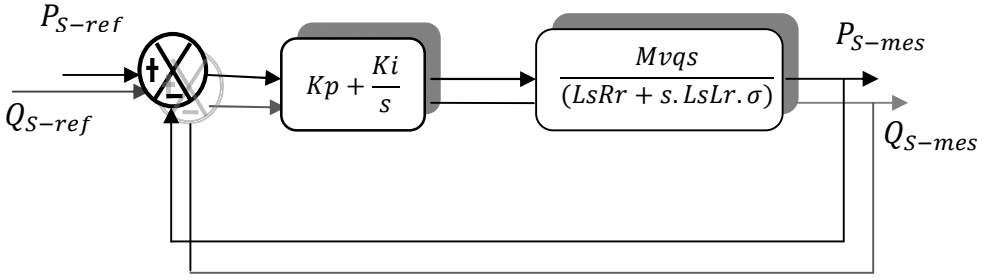

Figure B.1: Block diagram of the stator power control system.

$$with \qquad \sigma = (1 - \frac{M^2}{L_s.L_r})$$

The open loop transfer function (F_{BO}) of the control system of figure (B.1) is written as follows:

$$F_{BO} = \frac{s + \frac{K_i}{K_P}}{\frac{s}{K_P}} . \frac{\frac{Mv_{qs}}{L_s L_r \sigma}}{\frac{R_r}{L_r \sigma} + s}$$

The method of pole compensation consists in eliminating the zero of the transfer function and this leads us to the following equality:

$$\frac{K_i}{K_P} = \frac{R_r}{L_r \sigma}$$

After the compensation, we get the function F_{BO} as follows:

$$F_{BO} = \frac{K_P M v_{qs}}{L_s L_r \sigma . s}$$

Which gives us the following closed loop transfer function:

$$F_{BF} = \frac{1}{1 + \tau . s}$$

With:

$$\tau = \frac{L_s L_r \sigma}{K_P M v_{qs}}$$

τest the response time of the system that is fixed in the order of 10 ms :

$$K_P = \frac{L_s L_r \sigma}{\tau M v_{qs}}$$

$$K_i = \frac{R_r L_s}{\tau M v_{qs}}$$

We apply the same method on:

- Currents loop

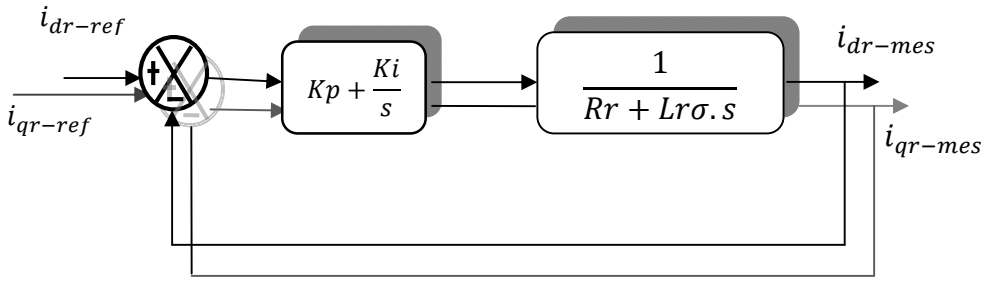

Figure B.2: Block diagram of the rotor current control system.

- Speed loop

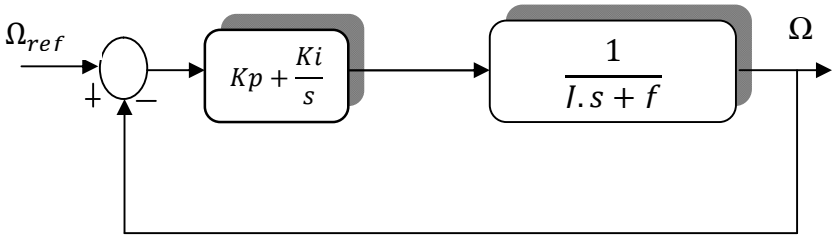

Figure B.3: Block diagram of the speed control system.

- Parameters of the classic PI regulators:

Power regulators	***Currents regulators***
K_P=*710.64*	K_P=200
K_i=8894.5	K_i=50

Table B.1: PI regulators parameters

.

Bibliography

[1] T. Burton, D. Sharpe, N. Jenkins, and E. Bossanyi, Wind Energy Handbook, Wiley, 2001.

[2] Adel Abdelbaset, Yehia S. Mohamed, Abou-Hashema M. El-Sayed, Alaa Eldin Hussein Abozeid Ahmed: Wind Driven Doubly Fed Induction Generator ‘‘Grid Synchronization and Control’’, Springer, 2018.

[3] “Renewables 2017 global status report,” REN21, 2017. [Online]. Available: http:// www.ren21.net/

[4] Son, J.-Y., & Ma, K. “Wind Energy Systems,” IEEE Trans. Power Electron., vol. 105, no. 11, pp. 2116–2131, Nov. 2017.

[5] REN21. (Jan. 2017). Renewables 2016: Global Status Report (GSR). [Online]. Available: http://www.ren21.net/.

[6] GWEC. (Feb. 2017). Global Wind Statistics 2016. [Online]. Available: www.gwec.net

[7] UpWind Project. (Mar. 2011). Design Limits and Solutions for Very Large Wind Turbines. [Online]. Available:http://www.ewea.org/fileadmin/ewea_documents/documents/upwind/21895_UpWind_Report_low_web.pdf

[8] Tajhau,“The Inside of a Wind Turbine,” Beijing: Mechanical Industry Press,2002

[9] L.L. Freries, Wind Energy Conversion Systems , Prentice Hall,1990.

[10] S.Heier, Grid Integration of Wind Energy Conversion Systems, Chapter 1, John Wiley & Sons Ltd, 1998.

[11] J.F. Manwell, J.G. McGowan, A.L. Rogers, Wind Energy Explained, Theory, Design and Application, Wiley, 2002.

[12] S. Mathew, Wind Energy Fundamentals, Resource Analysis, and Economics, Springer, 2006.

[13] S. Heier, Grid Integration of Wind Energy Conversion Systems, Chicester, U.K.: Wiley, 2nd Edition, 2006.

[14] T. Ackermann, Wind Power in Power Systems, John Wiley & Sons, 742 pages, Jan. 2005.

[15] M.R. Patel, Wind and Solar Power Systems, New York, USA: CRC Press, 368 pages, Mar 1999.

[16] G. L. Johnson. Wind Energy Systems. Prentice-Hall, Englewood Cliffs, New Jersey, 1985.

[17] Wind Resource Map of a Section of New Brunswick (http://www2.gnb.ca/content /dam/gnb/ Departments/ en/pdf/MapsCartes/CarteSpd_80m_nb_en_tuile_05_06.pdf)

[18] Averaged Wind Speed Data (Environment Canada) (https://www.halifax.ca/ regional planning/documents/ FigureA14AverageWindSpeed.pdf)

[19] A. Kulka, “Pitch and Torque Control of Variable Speed Wind Turbines”, M.Sc. thesis, Chalmers University of Technology, Goteborg, Sweden, 2004.

[20] T. Petru, “Modelling of Wind Turbines for Power System”, Lic. thesis, Chalmers Univer-sity of Technology, Goteborg, Sweden, 2001.

[21] O. Alizadeh, “Control of Wind Energy Conversion Systems for Large-Scale Integration with the Power System”, Phd. thesis, The University of Western Ontario, 2014.

[22] A. Tanvir, “Control System for Doubly Fed Induction Generator Based Wind Energy Conversion”, M.Sc. thesis, Saint Mary’s University, Halifax, Canada, 2016.

[23] G. L. Johnsson, Wind Energy Systems. Englewood Cliffs, N.J., USA.: Prentice-Hall, 1985.

[24] B.Wu, Y. Lang, N. Zargari, S. Kouro, Power Conversion and Control of Wind Energy System, Wiley, IEEE Press, 2011.

[25] M. P. Papadopoulos, S. A. Papathanassiou, N. G. Boulaxis, and S. T. Tentzerakis, “Voltage quality change by grid-connected wind turbines,” in European Wind Energy Conference, Nice, France, 1999, pp. 783–785.

[26] T. Petru and T. Thiringer, “Active flicker reduction from a sea-based 2.5 MW wind park connected to a weak grid,” in Proc. Nordic Workshop on Power and Industrial Electronics, Aalborg, Denmark, June, 13–16, 2002.

[27] A. Larsson, P. Sørensen, and F. Santjer, “Grid impact of variable speed wind turbines,” in Proc. of European Wind Energy Conference and Exhibition (EWEC´99), Nice, France, Mar., 1–5, 1999

[28] F. Blaabjerg and Z. Chen, Power Electronics for Modern Wind Turbines, Morgan & Claypool Publishers, 2006.

[29] D. Burnham, S. Santoso, and E. Muljadi, Variable Rotor-Resistance Control of Wind Turbine Generators, in IEEE Power and Energy Society General Meeting (PES), 2009.

[30] http://www.ianswer4u.com/2012/02/wind-energy advantagesand.html #axzz3Qs5RV0Sb

[31] Eduard Muljadi, M. Singh, and V. Gevorgian, “Doubly Fed Induction Generator in an Offshore Wind Power Plant Operated at Rated V/Hz”, Energy Conversion Congress and Exposition (ECCE), Raleigh, NC, USA, pp. 779-786, 15-20 September. 2012.

[32] S. Muller, M. Deicke and RikW. De Doncker, “Doubly fed induction generator systems for wind turbines,” IEEE, Industry Applications Magazine, vol. 8, issue. 3, pp. 26-33, May/June 2002.

[33] Paul C. Krause, “Analysis of Electric Machinery”, McGraw-Hill, Inc.City and State, 1986.

[34] M. Aktarujjaman, M.E. Haque, and K. M. Muttaqi, “Control Dynamics of a Doubly Fed Induction Generator Under Sub- and Super-Synchronous Modes of Operation,” IEEE PES General Meeting, Pittsburgh, PA, USA, pp. 1- 9, July 20-24. 2008.

[35] MICHAEL A. SNYDER“Development of Simplified Models of Doubly-Fed Induction Generators” M.Sc. thesis, Chalmers Univer-sity of Technology, Goteborg, Sweden, 2012.

[36] Tarek Masaud, “Modeling, Analysis, Control and design application guidelines of doubly fed induction generator (DFIG) for wind power applications” Phd. thesis, The University of Golden, Colorado, 2014.

[37] Srirattanawichaikul,W, Kumsuwan Y, Premrudeepchacharn S, and Wu B, “A Vector Control of A Grid Connected 3L-NPC-VSC with DFIG Drives,” (ECTI-CON) International Conference, Chiang Mai, Thailand, pp. 828-832, May. 2010.

[38] « Commande vectorielle et adaptative de la MADA » Mémoire d’ingénieur. Université de Batna [2002]

[39] Cardenas, R. Pena, R. Proboste, J. Asher, G. Clare, J. ‘’MRAS Observer for Sensorless Control of Standalone Doubly Fed Induction Generators’’ IEEE Transactions on Energy Conversion, Vol. 20, No 4 , pp. 710 – 718,05 Dec 2005,

[40] Yuan Guofeng; Li Yongdong; Chai Jianyun; Jiang Xinjian; ‘’A Novel Position Sensor-less Control Scheme of Doubly Fed induction Wind Generator Based on MRAS Method ‘’ IEEE Power Electronics Specialists Conference, PESC .2008.,pp. 2723 – 2727.

[41] Dendouga, R. Abdessemed, M. L. Bendaas and A. Chaiba" Decoupled Active and Reactive Power Control of a Doubly-Fed Induction Generator (DFIG). Proccedings of the 15th mediterrance conference on control &Automation, july ,2007,Athens-Greec.

[42] Cardenas, R. Peiia, J. Proboste , G. Asher, J. Clare ‘’Sensorless Control of a Doubly- Fed Induction Generator for Stand Alone Operation’’ The 30th Annual Conference of the IEEE Industrial Electronics, 2004, pp. 0275-9306.

[43] Nait-kaci, B. Doumbia, M.L. Agbossou, K. Yousif, A. ‘’active and reactive power control of a doubly fed induction generator for wind applications’’ IEEE EUROCON 2009,pp. 2034 – 2039.

[44] Pea, R, Cerdenas, R, Proboste, J, Asher, G., Clare, J‘’Sensorless Control of Doubly-Fed Induction Generators Using a Rotor-Current-Based MRAS Observer ‘’ IEEE Transactions on Industrial Electronics, Vol. 55, no. 1, pp. 330 - 339, January 2008.

[45] Ghennam, T. Berkouk, E.M. Francois, B. ‘’modeling and control of a doubly fed induction generator (DFIG) based wind conversion system ’ IEEE Power Engineering, Energy And Electrical Drives Specialists Conference,.2009.,pp. 507 - 512.

[46] D.Aouzellag, K.Ghedamsi , E.M.Berkouk ‘’Network Power Flow Control of Variable Speed Wind Turbine’ IEEE Power Engineering, Energy And Electrical Drives Specialists Conference,.2007.,pp. 435 – 439.

[47] Baike Shen; Mwinyiwiwa, B., Yongzheng Zhang, Boon-Teck Ooi, British Columbia Transm. Corp, Vancouver, BC ‘’Sensorless Maximum Power Point Tracking of Wind by DFIG Using Rotor Position Phase Lock Loop(PLL) ‘’ IEEE Transactions on Power Electronics, vol. 24, no. 4,pp. 942 – 951, April 2009.

[48] Brahmi, J. Krichen, L. Ouali, A. ‘’sensorless control of PMSG in wecs using artificial neural network’’ Systems, Signals and Devices, 2009. SSD '09. 6th International Multi-Conference on.,pp. 1 - 8

[49] J. S. Thongam , P. Bouchard, H. Ezzaidi and M. Ouhrouche ‘’Wind Speed Sensorless Maximum Power Point Tracking Control of Variable Speed Wind Energy Conversion Systems’’IEEE Machines and Drives International Conference, 2009, pp. 1832 – 1837.

[50] M.B.Mohamed, M.Jemli, M-Gossa, K. Jemli." Doubly fed induction generator (DFIG) in wind turbine modelling and power flow control ‘’ IEEE International Conference on Industrial Technology (ICIT), 2004.

[51] F. Poitiers, M. Machmoum, R. Le Doeuff and M.E. Zaim’’ control of a doubly-fed induction generator for wind energy conversion systems ‘’ the 44th International Conference Universities Power Engineering (UPEC), 2009, pp. 1 – 5.

[52] Farrokh Payam, and M. Jalalifar ‘’ Robust Speed Sensorless Control of Doubly-Fed Induction Machine Based on Input-Output Feedback Linearization Control Using a Sliding-Mode Observer’’ Proceedings of the IEEE International Conference on Power Electronics, Drives and Energy Systems, pp. 1 - 5 ,2006.

[53] Cardenas, R. Pena, R. Proboste, J. Asher, G. Clare, J. ‘’MRAS Observer for Sensorless Control of Standalone Doubly Fed Induction Generators’’ IEEE Transactions on Energy Conversion, Vol. 20, No 4 , pp. 710 – 718,05 Dec 2005.

[54] Sönke Thomsen, Kai Rothenhagen, Friedrich W. Fuchs ‘’Online Parameter Identification Methods for Doubly Fed Induction Generators’’ IEEE Power Electronics Specialists Conference, PESC pp. 2735 – 2741, 15-19 June 2008.

[55] Carles Batlle, Arnau Doria-Cerezo and Romeo Ortega’’A Stator Voltage Oriented PI Controller For The Doubly-Fed Induction Machine’’Proc of the American Control Conference New York City, USA, July 11-13, 2007.

[56] Eric Maldonado, C´ esar Silva, Manuel Olivares ‘Sensorless Control of a Doubly Fed Induction Machine Based on an Extended Kalman Filter’ Proc IEEE Power Electronics and Applications ,pp.1 – 10, 30 Aug-1 Sept . 2011.